NASA TECHNICAL NOTE

NASA TN D-6795

OXIDATION AND THERMAL FATIGUE OF COATED AND UNCOATED NX-188 NICKEL-BASE ALLOY IN A HIGH-VELOCITY GAS STREAM

by James R. Johnston and Stanley G. Young

Lewis Research Center
Cleveland, Ohio 44135

NATIONAL AERONAUTICS AND SPACE ADMINISTRATION • WASHINGTON, D. C. • MAY 1972

1. Report No.	2. Government Accession No.	3. Re
NASA TN D-6795		

4. Title and Subtitle	5. Report Date
OXIDATION AND THERMAL FATIGUE OF COATED AND UNCOATED NX-188 NICKEL-BASE ALLOY IN A HIGH-VELOCITY GAS STREAM	May 1972
	6. Performing Organization Code
7. Author(s)	8. Performing Organization Report No.
James R. Johnston and Stanley G. Young	E-6778
	10. Work Unit No.
9. Performing Organization Name and Address	134-03
Lewis Research Center National Aeronautics and Space Administration Cleveland, Ohio 44135	11. Contract or Grant No.
	13. Type of Report and Period Covered
12. Sponsoring Agency Name and Address	Technical Note
National Aeronautics and Space Administration Washington, D. C. 20546	14. Sponsoring Agency Code

15. Supplementary Notes

16. Abstract

A cast nickel-base superalloy, NX-188, coated and uncoated, was tested in a high-velocity gas stream for resistance to oxidation and thermal fatigue by cycling between room temperature and 980°, 1040°, and 1090° C. Contrary to the behavior of more conventional nickel-base alloys, uncoated NX-188 exhibited the greatest weight loss at the lowest test temperature. In general, on the basis of weight change and metallographic observations a coating consisting of vapor-deposited Fe-Cr-Al-Y over a chromized substrate exhibited the best overall performance in resistance to oxidation and thermal fatigue.

17. Key Words (Suggested by Author(s))	18. Distribution Statement
Oxidation; Thermal fatigue; Coatings; NX-188; Nickel-base alloys; Electron microprobe; High-gas-velocity burner	Unclassified - unlimited

19. Security Classif. (of this report)	20. Security Classif. (of this page)	21. No. of Pages	22. Price*
Unclassified	Unclassified	40	$3.00

* For sale by the National Technical Information Service, Springfield, Virginia 22151

OXIDATION AND THERMAL FATIGUE OF COATED AND UNCOATED NX-188 NICKEL-BASE ALLOY IN A HIGH-VELOCITY GAS STREAM

by James R. Johnston and Stanley G. Young

Lewis Research Center

SUMMARY

An investigation was conducted to determine the oxidation and thermal fatigue resistance of the cast nickel-base superalloy NX-188, coated and uncoated, during cyclic heating in a high-velocity gas stream. Specimen temperatures of 980° C, 1040° C, and 1090° C were generated with a natural-gas burner having an exit velocity of Mach 1. Three coatings were evaluated: slurry-applied Fe-Cr-Al-Y, duplex Cr/Al, and vapor-deposited Fe-Cr-Al-Y over Cr. In order to observe effects of specimen geometry, both the NASA wedge specimen and the Pratt & Whitney erosion bar were used. Evaluation was based on weight change, thermal cracking, and metallographic observations.

Uncoated specimens of both shapes exhibited greater weight loss at 980° C than at 1040° C and 1090° C. At the two higher temperatures, uncoated NX-188 compared favorably with representative nickel-base alloys tested in a previous investigation.

Based on the weight change during 100-hour tests, all the coatings were satisfactory at 980° C, showing a gradually increasing weight throughout the test. At 1040° C some coated specimens started to lose weight during the 100-hour test. At 1090° C only the Cr/vapor-deposited Fe-Cr-Al-Y coating provided good protection on both types of specimens.

The thermal fatigue resistance of coated and uncoated specimens was relatively good compared with previous tests with representative uncoated nickel-base alloys. No cracks were noted on any specimens after the tests at 980° and 1040° C or on the vapor-deposited Fe-Cr-Al-Y coated specimens at 1090° C. In previous tests almost all uncoated cast nickel-base alloy specimens cracked in less than 100 hours at similar temperatures.

The protection afforded by the coatings seemed to depend upon the formation of aluminum-bearing surface scales and the limitation of diffusion of the base metal elements, nickel and molybdenum, to the surface. The differences in performance of the specific coatings were considered to be due in part to the significant differences in coating thickness.

INTRODUCTION

The rate of development of the gas turbine engine has generally been limited by the high-temperature alloys available for the turbine vanes and blades. Materials suitable for use as turbine vanes have until recently been restricted to conventional cast nickel-base and cobalt-base alloys. Cobalt alloys have generally been preferred for stator vanes due to their higher melting point, greater resistance to sulfidation, and better thermal fatigue behavior. However, cobalt alloys are limited by relatively low strength, as well as poor oxidation resistance at temperatures above 900° C. Dispersion-strengthened alloys such as TD-Ni and TD-NiCr have also been considered for vane applications, but high cost and difficult fabricability have limited the use of these materials.

The development of a unique alloy based on the nickel-aluminum-molybdenum system has been reported in the last two years (ref. 1). The alloy, NX-188, has a high melting point (1300° to 1315° C), creep strength above 1090° C superior to most other cast nickel-base alloys, good castibility, and excellent stability. Since oxidation resistance is marginal, coating is necessary. On the basis of such preliminary studies as reported in reference 1, NX-188 appeared to have most of the characteristics required for a vane material. Little information was available, however, on the thermal fatigue resistance of the alloy or on the performance of the alloy and coating systems when exposed to the high-gas-velocity oxidation conditions encountered in gas turbine engines.

In order to provide additional performance data which would permit more complete evaluation of the alloy, coated and uncoated specimens of NX-188 were exposed to cyclic oxidation in a high-gas-velocity facility (ref. 2) at the Lewis Research Center. In order to observe effects of specimen geometry, two specimen types were used, the NASA wedge specimen and the Pratt & Whitney erosion bar. Tests were conducted at temperatures of 980°, 1040°, and 1090° C. The coatings evaluated were a slurry-applied Fe-Cr-Al-Y, pack-cementation duplex Cr/Al, and vapor-deposited Fe-Cr-Al-Y over pack-cementation Cr. The tested specimens were evaluated on the basis of weight change, thermal fatigue cracking, and microstructural effects as determined by metallography and electron probe analyses.

MATERIALS, APPARATUS, AND PROCEDURE

Specimens

The two specimen configurations used in this investigation are shown in figure 1. The NASA specimen was 10.6 centimeters by 2.54 centimeters by 0.63 centimeter and was tapered along one long edge with a 45° included angle and an 0.8-millimeter radius.

The Pratt & Whitney specimen (ref. 3) was basically a 1.27-centimeter-diameter round with two flats along the length at an included angle of 30°.

Uncoated and coated specimens were supplied by the developers of the alloy NX-188. All specimens had been cast by a commercial vendor from NX-188 alloy having the following nominal composition by weight percent:

Nickel	Molybdenum	Aluminum	Carbon
Bal	18	8	0.04

Typical chemical analyses from specimens of the alloy used in this investigation were as follows (obtained from independent laboratory):

Nickel	Molybdenum	Aluminum	Carbon
74.12	17.62	8.20	0.037
74.05	17.62	8.32	.047

The specimens were tested in the uncoated condition and with the following three coatings:

(1) Slurry-applied Fe-Cr-Al-Y

(2) Pack-applied Cr/Al duplex

(3) Vapor-deposited Fe-Cr-Al-Y over pack-applied Cr.

The slurry used to apply the Fe-Cr-Al-Y coating of item (1) contained a small amount of silicon to promote densification during sintering. The Cr/Al duplex coating was applied in two steps, aluminum over chromium. The vapor-deposited Fe-Cr-Al-Y was applied to specimens which had been precoated with chromium by pack cementation.

High-Gas-Velocity Oxidation Apparatus

The burner used to expose the specimens to high velocity gas is shown in figure 2. The photograph illustrates the general configuration of the burner and the rotating specimen holder. The specimens were mounted on a rotating fixture that was moved vertically between heating and cooling positions by an air cylinder. In the heating position the specimens were partially surrounded by a segmented cylindrical radiation shield. The shield helped to minimize the lengthwise and chordwise temperature gradients within the specimens.

The burner used natural gas and compressed air to generate exit gas temperatures as high as 1550° C with gas velocities of Mach 1. The design of the burner minimized

heat losses; hence, the fuel/air ratio was as lean as possible. A more detailed description of the burner equipment is given in reference 2.

The two types of specimen holder assemblies used are shown in figure 3. Each holder had provision for eight specimens. The major differences between the assemblies were the retaining methods used and the length of specimen exposed to the burner gas. The Pratt & Whitney specimen had approximately 5 centimeters of heated length, while the NASA specimen had about $7\frac{1}{2}$ centimeters exposed.

In each case the temperature of the specimens was monitored with an optical pyrometer which was periodically calibrated by comparison with a thermocouple imbedded in a dummy specimen. The burner gas temperature was controlled with an automatic closed-loop system which maintained the specimen temperature within $\pm 8^{\circ}$ C of the nominal test temperature.

Test Conditions

The burner test conditions used in this program are shown in table I. The specimens were alternately heated for 1 hour at the specified test temperature and cooled for 3 minutes to room temperature. Each test was continued for 100 hours. The burner chamber pressure was maintained slightly above 2 atmospheres (0.2 MN/m^2) to provide an exit gas velocity of Mach 1. The cooling air jet velocity was also Mach 1.

Test Procedure

Prior to testing, the specimens were degreased in trichlorethylene vapor and weighed on an analytical balance with a precision of 0.2 milligram. At intervals of 20 hours of testing the specimens were removed from the apparatus, reweighed, photographed, and inspected for cracks with fluorescent dye penetrant. Before further testing they were again degreased.

Most test runs were conducted with two uncoated specimens and two specimens with each of the three coatings, making a total of eight specimens. In the case of the NASA specimens, enough were available with the vapor-deposited Fe-Cr-Al-Y coating to permit testing only at the highest temperature, 1090° C.

After exposure to the burner, specimens were prepared for metallographic examination and electron microprobe studies as described in detail in the following section. Samples of surface oxides for X-ray diffraction analyses were scraped from the areas of maximum temperature at the tapered edge of the NASA specimens.

Metallographic Specimen Preparation

After testing, the oxidation specimens were prepared for metallographic and electron microprobe studies as follows. Most tested specimens were copper plated. First, a copper coating was vapor deposited over the oxidized specimen. Then, more copper was added by electroplating until the copper coating reached a thickness of about 0.5 millimeter. The oxidized ends of the specimens were then encapsulated in epoxy, sectioned transversely at the zone of maximum test temperature, and polished metallographically. A 33-percent acetic acid, 33-percent nitric acid, 33-percent water, and 1-percent hydrofluoric acid etchant was used; and optical photomicrographs were taken. The specimens were then repolished on a diamond-impregnated cloth wheel. Finally, for electron microprobe specimens, a copper film was vapor deposited on the cut and polished specimens to provide a conductive path to ground for the electrons of the incident beam as it traversed nonconducting phases. Electron backscatter and individual element X-ray raster photographs were taken. Line traverses were made by moving the specimen linearly under the beam and continuously recording X-ray intensity to provide semiquantitative composition information.

RESULTS AND DISCUSSION

Weight Change

The results of the weight change measurements are shown in figure 4 for coated and uncoated NX-188 specimens. Data are presented for both the NASA and the Pratt & Whitney specimen configurations. The uncoated specimens all exhibited substantial weight loss after 100 hours. The greatest weight loss for both types of specimens occurred at the lowest temperature, 980° C. This anomaly may indicate that, at the lowest test temperature, the inhibiting effect of aluminum on the formation of molybdenum trioxide suggested in reference 1 was not as pronounced as it was at the higher temperatures. At the higher temperatures the effectiveness of the aluminum in providing protection was manifested not only in the substantial reduction in weight loss but also in the promoting of smoother, more adherent oxide scales. Significant differences in the appearance of the NASA specimens tested at different temperatures are apparent in figure 5. The specimens tested at 1040° C, and to a lesser extent those at 1090° C, were markedly smoother than the specimens tested at 980° C. The minimum weight loss of the NASA specimens occurred at the intermediate temperature 1040° C (fig. 4(b)), while that of the Pratt & Whitney specimens occurred at 1090° C (fig. 4(f)). The reason for

this difference is not obvious, but it is believed that specimen geometry and the resulting difference in temperature distribution was a major factor.

The weight loss results for the uncoated NASA specimens are compared in figure 6 with representative nickel-base alloys tested in the investigation of reference 2. It is apparent that at the higher temperatures, 1040° to 1090° C, the performance of uncoated NX-188 compares favorably with that of the other alloys. At the lowest temperature of 980° C, however, the uncoated NX-188 specimens were extremely poor relative to the nickel-base alloys. At this temperature the performance was comparable to that of one of the least oxidation-resistant cobalt alloys, WI-52.

The relative performance of the coated specimens regardless of specimen type was strongly dependent on temperature. At the lowest temperature, 980° C (figs. 4(a) and (d)), essentially no difference was noted among the coatings in the 100-hour tests; all coated specimens produced relatively smooth weight-gain curves approximating parabolic oxidation behavior. At 1040° C the Cr/Al coated NASA specimens (fig. 4(b)) and the Fe-Cr-Al-Y (slurry) coated Pratt & Whitney specimens (fig. 4(e)) started to lose weight during the 100-hour tests. At 1090° C (figs. 4(c) and (f)) only the Cr/vapor-deposited Fe-Cr-Al-Y coating prevented weight loss on both types of specimens and thus showed the best overall performance. However, it should be noted that the thicknesses of the three coatings were considerably different. The estimated total thickness of Fe-Cr-Al-Y (slurry), Cr/Al pack, and Cr/vapor-deposited Fe-Cr-Al-Y coatings were 100, 190, and 280 micrometers, respectively. It is probable that the differences in protection afforded by the various coatings were due in part to these large differences in thickness.

As in the case of the uncoated specimens, some differences in coating performance were observed with the two specimen shapes. The major difference noted was in the performance of the Cr/Al coating. For instance, in tests at 1090° C, NASA specimens with the Cr/Al coating showed appreciably higher weight loss than specimens with the other coatings (fig. 4(c)), while Pratt & Whitney specimens with the Cr/Al coating did not lose weight during the 100-hour test and hence were equal to or better than those with the other coatings (fig. 4(f)). The reason for this anomalous behavior is not obvious. Metallographic examination of each type of specimen after testing revealed nothing which could account for the difference in performance between the two types of specimens. It is believed to result, as in the case of the uncoated specimens, from the difference in the specimen geometry and the corresponding difference in temperature distribution.

Thermal Fatigue Cracking

A summary of the thermal fatigue results is shown in table II for the uncoated and coated NX-188 specimens of the NASA configuration. No cracks were noted on any

NX-188 specimens after 100 hours at 980° or 1040° C or on the Cr/vapor-deposited Fe-Cr-Al-Y coated specimen at 1090° C. The thermal fatigue resistance demonstrated by both the coated and uncoated specimens was quite good compared with results from a previous study (ref. 2) made with other uncoated nickel-base alloys. In that study almost all the alloys tested at these temperatures cracked in less than 100 hours, and many cracked in 20 to 40 hours.

The shape of the Pratt & Whitney specimens precluded the generation of thermal stresses high enough to cause thermal fatigue cracking in the test times investigated.

X-Ray Diffraction

Table III lists the oxides identified by X-ray diffraction of scales scraped from coated and uncoated specimens of NX-188 after 100-hour exposure to high-gas-velocity oxidation at various temperatures. The uncoated NX-188 alloy specimens generally produced NiO, Al_2O_3, and a spinel with a lattice spacing a_o of 8.05×10^{-10} meter, except at 1090° C where no Al_2O_3 was detected. The coatings all produced scales containing Al_2O_3. The monoxide, NiO, appeared on specimens with the Fe-Cr-Al-Y (slurry) coating tested at 1090° C and the Cr/Al coatings tested at 980° and 1090° C. Cr_2O_3 was detected only on the specimens with the Cr/vapor-deposited Fe-Cr-Al-Y coating.

Light Metallography

Microstructure of as-received specimens. - Typical microstructures of as-received specimens are shown in figure 7. The micrographs of figures 7(a) to (c) are transverse sections of the leading edge of the NASA specimens. The micrograph of figure 7(d) is from the smaller arc of the 1.27-centimeter-diameter portion of a Pratt & Whitney specimen. The uncoated NASA specimen (fig. 7(a)) showed a typical cast structure out to the edge. In the Fe-Cr-Al-Y (slurry) coated specimen (fig. 7(b)), three phases are evident in the coarse-structured outer zone and two phases in the fine-structured inner (diffusion) zone. The diffusion zone is defined as the zone directly above the base metal in which coating elements can be detected. The Cr/Al coated specimen (fig. 7(c)) shows three fine-structured zones. Each zone seems to be composed of at least two phases. The Fe-Cr-Al-Y (vapor deposited) coated specimen (fig. 7(d)) shows six zones above the base metal. The wide outer zone appears to be a single phase. Large precipitates can be observed at the diffusion zone - base metal interface.

Microstructure of as-tested specimens. - Micrographs of transverse sections of the leading edges of tested NASA specimens cut through the hot zone are shown in figure 8. Similar studies were made of the Pratt & Whitney specimens, and all were

similar in structure to the NASA type. Figures 8(a) to (c) show uncoated NX-188 specimens after 100-hour exposures at 980°, 1040°, and 1090° C, respectively. In figure 8 and all subsequent micrographs, the oxide scale is near the top of the micrograph. When copper plating was used, the added layers of copper are evident above the oxide scale. (This layer is indicated in fig. 8(b); the specimens in figs. 8(a) and (c) were not copper coated.) The copper coating was used to preserve the oxide and to allow electron microprobe examination at the specimen surface. Below the oxide scale was an Al depletion zone as verified by the electron microprobe. This zone widened with increasing temperature.

Figures 8(d) to (f) show the Fe-Cr-Al-Y (slurry) coated NX-188 specimens after 100-hour exposures at 980°, 1040°, and 1090° C, respectively. An oxide scale and three zones containing several different metallic phases were observed. The three-phase zone of the as-received specimen (fig. 7(b)) changed to a one- or two-phase zone, and the fine-structured diffusion zone coarsened. The interface between coating and substrate was not so sharply delineated after testing.

The Cr/Al coated specimens are shown in figures 8(g) to (i) after exposure at 980°, 1040°, and 1090° C, respectively. The coatings, when compared to the fine-structured as-received coatings (fig. 7(c)), show significant coarsening and a larger-grained structure. The 980° and 1040° C coatings are similar in appearance, but the 1090° C coating showed a severely irregular outer surface.

The Cr/vapor-deposited Fe-Cr-Al-Y coated specimen run at 1090° C is shown in figure 8(j). This coating when compared to that on the unexposed specimen (fig. 7(d)) also showed a coarsening of the coating structure with exposure. A sharp interface was noted between the diffusion zone and the base metal of the test specimen.

Electron Microprobe X-Ray Analyzer Studies

Electron microprobe backscatter and X-ray raster micrographs were taken for metallic elements at the leading edges of selected NASA specimens exposed to various conditions. Typical examples are given in figures 9 to 11. Line traverses were also made at the leading edges of each of these specimens and are shown in the appendix in figures 12 to 16. The discussion of the electron microprobe micrographs is included with the explanation of the traverse results for each specimen type in the appendix.

Uncoated specimens - Uncoated specimens tested at 980° and 1090° C showed a porous, discontinuous scale at the surface that contained Ni and Al, but no Mo. X-ray results indicated the presence of a spinel which was probably $NiAl_2O_4$. A less porous scale containing higher Al (probably Al_2O_3) was observed on the 1040° C specimen which showed significantly less weight loss than specimens tested at either of the other two

temperatures. An Al-depleted zone, which was high in Mo and Ni relative to the base metal and which widened with exposure temperature, was observed above the base metal at all temperatures.

Fe-Cr-Al-Y (slurry) coated specimens. - The diffusion zone of the Fe-Cr-Al-Y (slurry) coated specimens widened from 980° to 1040° C but remained the same from 1040° to 1090° C. An external high-Al-content scale was observed which decreased in Al content with increasing temperature. The 1090° C specimen, which had a weight loss after 100 hours of testing, lacked a clearly defined Al depletion zone such as that observed beneath the scales of the specimens tested at 980° and 1040° C.

Cr/Al coated specimens. - The fine structure of the as-received Cr/Al coated specimens coarsened after exposure. The oxide scale in all cases was high in aluminum. An Al depleted zone beneath the oxide was observed at 980° and 1040° C but not at 1090° C. A high-Cr-content zone was observed directly beneath the Al depleted zone at the lower two test temperatures, but at 1090° C it was directly beneath the oxide scale. Attack of this zone (as indicated by the irregular surface (fig. 8(i))) could account for the high weight loss observed at 1090° C.

Cr/vapor-deposited Fe-Cr-Al-Y coated specimens. - In the very thick vapor-deposited Fe-Cr-Al-Y coating, a general coarsening of the structure was observed after exposure. A high-Al-content (Al_2O_3) scale was observed. A large increase in Ni, a small increase in Mo, and a decrease in Al were observed in the zone directly beneath the oxide scale, while Cr and Fe content in this same zone of the exposed specimen remained nearly the same as in the as-received specimen. However, these elements diffused into the base metal. It appears that the protection afforded the NX-188 substrate by the Cr/vapor-deposited Fe-Cr-Al-Y coating, as well as the other two coatings, depends upon the formation of Al-bearing surface scales. In the case of the Cr/vapor-deposited Fe-Cr-Al-Y coating, the thickness of the coating appeared to limit the diffusion of Mo and Ni outward to the surface.

SUMMARY OF RESULTS

An investigation was conducted to determine the oxidation and thermal fatigue resistance of the nickel-base superalloy NX-188, coated and uncoated, during cyclic exposure to a high-velocity gas stream. A compressed-air - natural-gas burner with exit gas velocity of Mach 1 was used to generate specimen temperatures of 980°, 1040°, and 1090° C. The coatings evaluated were slurry-applied Fe-Cr-Al-Y, pack-cementation duplex Cr/Al, and vapor-deposited Fe-Cr-Al-Y over pack-cementation Cr. In order to observe effects of specimen geometry, two specimen shapes were used - the NASA wedge, which generates high thermal stresses; and the Pratt & Whitney bar, which is intended primarily for the study of corrosion. The following results were obtained:

1. Uncoated specimens of both shapes exhibited greater weight loss at 980° C than at 1040° or 1090° C. At the two higher temperatures, the performance of NX-188 compared favorably with representative uncoated nickel-base alloys tested in a previous investigation.

2. All the coatings tested at 980° C showed a weight gain approximating parabolic behavior throughout the 100-hour test. At 1040° C the Cr/Al coated NASA specimens and the Fe-Cr-Al-Y (slurry) coated Pratt & Whitney specimens started to lose weight during the 100-hour test. At 1090° C only the Cr/vapor-deposited Fe-Cr-Al-Y coating prevented weight loss on both types of specimens and in general showed the best overall performance.

3. The thermal fatigue resistance determined with both coated and uncoated NASA specimens was quite good compared to previous tests with representative uncoated nickel-base alloys. For instance, in 100 hours no cracks were noted on any NX-188 specimens at 980° or 1040° C or on the vapor-deposited Fe-Cr-Al-Y coated specimen at 1090° C. In previous tests, almost all uncoated, conventionally cast, nickel-base alloys tested at 980°, 1040°, and 1090° C cracked in less than 100 hours; and many cracked in 20 to 40 hours.

4. The protection afforded the NX-188 alloy by the coatings seemed to depend upon the formation of Al-bearing surface scales and the limitation of diffusion of the base metal elements, Ni and Mo, to the surface. The differences in performance of the specific coatings was considered to be due in part to the significant differences in coating thickness.

Lewis Research Center,
National Aeronautics and Space Administration,
Cleveland, Ohio, March 7, 1972,
134-03.

APPENDIX - ELECTRON MICROPROBE X-RAY ANALYZER (EMXA) STUDIES

Method of Representing Electron Microprobe Data

Electron microprobe traverse records are often long, irregular, and difficult to reproduce in print. Furthermore, a traverse may miss significant phases. A typical example of a short portion of a strip-chart record is given in figure 12. To more clearly visualize the elemental content of specimens, the schematic diagrams shown in figures 13 to 16 have been constructed. These figures show the average intensity ratios of each element based on estimations from the original charts as well as on interpretation from X-ray raster, light, and backscatter micrographs. The X-ray count rate of a high-purity standard for each element was compared with the count rate of each element in the alloy. The ratio of the count rate of the unknown to that of the standard, called the intensity ratio, is roughly equivalent to the weight percent of the element present. However, these data are only in terms of X-ray counts and have not been corrected for such effects as background, adsorption, fluorescence, and atomic numbers. Percent levels shown are, therefore, only semiquantitative and in some cases shown here may have an error as high as 20 percent absolute. In these plots two- or three-phase zones have been idealized, showing precipitates evenly distributed and of the same size within each zone. This, of course, is not the true situation, but the approximate composition of each phase and similarities between different specimens can be visualized more readily when presented in this manner. The relative size of precipitates can also be inferred from the width of the phases drawn in each zone.

A light photomicrograph of each specimen has been inserted at the top of each graph in figures 13 to 16 so that EMXA results may be related to the metallographic structures of the specimens.

Uncoated NX-188 Specimens

Figures 13(a) to (c) are the schematic EMXA concentration profiles for uncoated specimens tested for 100 hours at 980°, 1040°, and 1090° C, respectively. On each specimen, a narrow oxide scale was observed which appears black in the light micrographs (figs. 8(a) to (c)) and backscatter electron micrographs (BSE) (fig. 9(a)). At 980° and 1090° C, 15- to 20-percent Ni and ~5-percent Al were observed in this scale; but for the specimen tested at 1040° C, ~28-percent Ni and ~28-percent Al were noted (figs. 13(a) to (c)). No Mo was observed in the scales in any of the specimens analyzed by EMXA (e.g., see fig. 9(d)).

Beneath the outer scale on specimens tested at 980° and 1090° C (figs. 13(a) and (c)) was a porous, discontinuous scale that contained about 50-percent Ni and less than

10 percent Al. On the specimen tested at 980° C, this region contained a mixture of oxides and metallic phases. However, because of the porosity of the scales, excessive scatter was observed in the measurements. This inner scale may be a spinel. X-ray results presented in table III indicated the presence of a spinel which is probably $NiAl_2O_4$. The porous scale was not observed in the 1040° C specimen (fig. 13(b)) by EMXA measurements, but a spinel was observed by X-ray measurements in all three cases. Under the scales an Al depleted zone was observed above the base metal at all three temperatures. No marked change in composition of the depletion zone with temperature was observed, but the zone widened from 15 micrometers to 30 micrometers with increasing test temperatures from 980° to 1090° C (figs. 13(a) to (c)).

The base metal beneath the Al depletion zone is represented in figure 13 and is typical of the alloy NX-188. The matrix ($\gamma + \gamma'$) is high in Ni and Al and low in Mo, while the interdendritic constituent distributed in the matrix is high in Mo and low in Ni and Al.

Differences observed in the composition of the same phases in the base metal of different specimens are due primarily to different specimen structures (e.g., different-sized precipitates in regions analyzed). These differences as shown in figures 13(a) to (c) are not, however, considered significant.

Fe-Cr-Al-Y (Slurry) Coated Specimens

Figure 14(a) is the schematic EMXA concentration profile for the as-received Fe-Cr-Al-Y (slurry) coated specimen; and figures 14(b) to (d) depict the coated specimens after testing for 100 hours at 980°, 1040°, and 1090° C, respectively. The Fe-Cr-Al-Y (slurry) coated specimens in the as-received condition showed two zones; a large-grained three-phase outer zone, and a fine-grained diffusion zone. The large-grained three-phase outer zone contained phases high in Mo, indicating considerable interdiffusion of elements. A sharp demarkation was noted between the base metal and the fine-structured zone into which Cr and Fe had diffused. Three metallic zones were noted after testing at 980° and 1040° C (figs. 14(b) and (c)); and an oxide scale was observed which was high in Al, probably present as Al_2O_3 (see fig. 10(b) and table III). The level of Al in the scale decreased with increasing test temperature. Beneath the scale an Al depletion zone was observed (designated by I in figs. 14(b) and (c)). At 1040° C Mo-rich precipitates were found in this zone. A larger-grained two-phase zone (II) directly beneath zone I was observed at 980° and 1040° C. At the higher temperature, 1090° C (fig. 14(d)), it appeared that the Al depletion zone (I) had become part of zone II.

In the large-grained two-phase zone (II), the matrix of the specimens tested at 980°, 1040°, and 1090° C consisted of ~70-percent Ni, 5- to 9-percent Al, and 3- to

11-percent Mo, with smaller amounts of the coating elements comprising the remainder. The particles are high in Mo and Si and low in Ni and Al. The distribution of the elements is shown qualitatively in figure 10.

Directly above the base metal in figures 14(b) to (d) there appears the fine-structured (diffusion) zone (III) into which Fe, Cr, and Si had diffused. This zone widened with exposure temperature between 980° and 1040° C. The sharp dividing line between this zone and the base metal (as observed in the as-received specimen) was not evident after testing at any temperature.

Cr/Al Coated Specimens

Figure 15(a) is the schematic EMXA concentration profile for the as-received Cr/Al coated specimen; and figures 15(b) to (d) are the profiles for the coated specimens after testing for 100 hours at 980°, 1040°, and 1090° C, respectively. The as-received specimen had a three-zone fine structure with at least two phases in each zone. Al was highest in the outer zone and Cr was highest in the intermediate zone. The diffusion zone contained large, very-high-Mo-content precipitates near the base metal interface.

After 100 hours of testing, a much coarser structure was observed at all three temperatures; and four zones were observed in addition to an oxide scale. In figures 15(b) to (d) these have been labeled I to IV, starting from the zone beneath the oxide scale. Zone III was not seen in the specimen tested at 980° C.

The oxide scale in all three cases was very high in Al, approximately 45 percent. About 5-percent Ni was observed in the scale of the 980° and 1040° C specimens. The oxide scale was thicker in the 1090° C specimen than in those tested at the two lower temperatures. No Cr and Mo were observed in the oxide scales in any specimens.

Zone I consisted primarily of large grains. At 980° and 1040° C (figs. 15(b) and (c)) a small-grained phase was mixed with the large grains. The large-grained phase had higher Ni and Al and lower Mo and Cr than the small-grained phase. The amount of Al in the large-grained phase of zone I decreased from ~12 percent at 980° C to ~6 percent at 1040° and 1090° C. Mo and Cr increased in this zone with testing temperature.

Zone II was a sharply delineated two-phase region which decreased in width with increasing temperature between 1040° and 1090° C (figs. 15(c) and (d)). The matrix was high in Ni and Al and low in Mo and Cr. The precipitates were high in Mo and low in Al and Ni. The Cr, although higher in the precipitates in the 980° and 1040° C specimens, was uniformly distributed in the 1090° C specimen.

Zone III was not evident in the 980° C specimen. At 1090° C this zone had nearly the same composition as zone I. The width of zone III increased with increasing test temperature between 1040° and 1090° C.

Finally, in zone IV (termed the Cr diffusion zone) Cr decreases across this two-phase region to zero at some depth within the specimen. The width of this Cr diffusion zone increased with increasing temperature. The matrix in this zone was high in Ni and Al and low in Mo, while the precipitates were high in Mo and low in Ni and Al. Cr was higher in the high-Mo-content phase than in the matrix in all cases.

Cr/Vapor-Deposited Fe-Cr-Al-Y Coated Specimens

Figure 16(a) shows the schematic EMXA trace for Cr/vapor-deposited Fe-Cr-Al-Y coated NX-188 in the as-received condition, and figure 16(b) is the trace of a specimen after it was tested for 100 hours at 1090° C. In the as-received specimen, six zones were noted: starting from the outside, zone I is a wide Fe-rich (Fe-Cr-Al-Y) outer layer; zone II is a high-Al-content zone with varying amounts of Ni, Cr, Al, and Fe; zone III is a two-phase zone high in Cr and Mo; zone IV is generally a single-phase zone of increasing Ni and decreasing Fe and Cr with a few widely scattered high Mo particles; zone V is a two-phase fine-grained zone; and zone VI is a two-phase coarse-grained zone. Cr and Fe diffusion were detected to a depth of 280 micrometers.

After testing this coated material for 100 hours of cyclic oxidation at 1090° C (fig. 16(b)), a general coarsening of the structure was observed and only four zones in addition to a high-Al-content oxide scale were distinguishable. Beneath the scale, the Fe-rich (Fe-Cr-Al-Y) zone (I) had increased significantly in Ni content, with a smaller increase in Mo. Al decreased in this zone. Near the surface, Cr and Fe in this zone remained nearly as high as in the as-received specimen. However, these elements diffused into the base metal during test exposure, as shown by their tapering off near the high-Al-content zone (II). Apparently, for the test time involved, the thickness of this coating provided enough Al to form a protective Al_2O_3 scale and also hindered the diffusion of Mo and Ni to the surface where they could oxidize. Zones III, IV, and V of the as-received specimen seemed to merge to a three-phase zone after test (zone III of fig. 16(b)). Cr and Fe were detected in this tested specimen to a depth of 460 micrometers.

REFERENCES

1. Maxwell, Douglas H.: The Development of an Advanced Turbine Vane Alloy. ASM Metal Eng. Quart., vol. 10, no. 4, Nov. 1970, pp. 42-54.

2. Johnston, James R.; and Ashbrook, Richard L.: Oxidation and Thermal Fatigue Cracking of Nickel- and Cobalt-Base Alloys in a High Velocity Gas Stream. NASA TN D-5376, 1969.

3. Danek, G. J.: State-of-the-Art Survey on Hot Corrosion in Marine Gas-Turbine Engines. Rep. MEL-32/65, Marine Engineering Lab., Mar. 1965. (Available from DDC as AD-461181.)

TABLE I. - TYPICAL BURNER CONDITIONS

[Specimen test cycle: 1 hr at maximum temperature, 3-min cool to room temperature.]

Maximum specimen temperature, ^{o}C	980 to 1090
Burner gas temperature, ^{o}C	1350 to 1550
Gas velocity	Mach 1
Burner pressure, MN/m^2	0.23
Specimen rotational speed, rpm	900
Burner airflow, kg/sec	0.41 to 0.45
Cooling airflow, kg/sec	0.23
Air/fuel ratio	20 to 30
Burner nozzle diameter, cm	5.1

TABLE II. - THERMAL FATIGUE CRACKING OF COATED AND UNCOATED NX-188 ALLOY EXPOSED TO HIGH-GAS-VELOCITY OXIDATION (NASA SPECIMENS)

Coating	Test temperature, ^{o}C		
	980	1040	1090
	Number of cycles to first crack		
None	>100 >100	>100 >100	40 >100
Fe-Cr-Al-Y (slurry)	>100 >100	>100 >100	60 >100
Cr/Al (pack)	>100 >100	>100 >100	80 >100
Cr/vapor-deposited Fe-Cr-Al-Y	Not tested	Not tested	>100 >100

TABLE III. - OXIDES DETERMINED BY X-RAY DIFFRACTION OF SCALE SCRAPED FROM COATED AND UNCOATED NX-188 ALLOY AFTER EXPOSURE TO HIGH-GAS-VELOCITY OXIDATION

(NASA SPECIMENS)

Test temperature, °C	Coating			
	None	Fe-Cr-Al-Y (slurry)	Cr/Al (pack)	Cr/vapor-deposited Fe-Cr-Al-Y
	Oxides found			
980	NiO (VS[a]) Spinel[b] (8.05) (S) Al_2O_3 (VW)	Al_2O_3 (W)	NiO (W) Al_2O_3 (W)	Not tested
1040	NiO (S) Spinel (8.05) (VW) Al_2O_3 (VW)	Al_2O_3 (S)	Al_2O_3 (VW)	Not tested
1090	NiO (VS) Spinel (8.05) (W)	NiO (VW) Al_2O_3 (W)	NiO (W) Al_2O_3 (M)	Al_2O_3 (S) Cr_2O_3 (W)

[a]VS very strong; S strong; M medium; W weak; VW very weak.
[b]Values in parentheses are lattice parameters in angstroms ($\times 10^{-10}$ m).

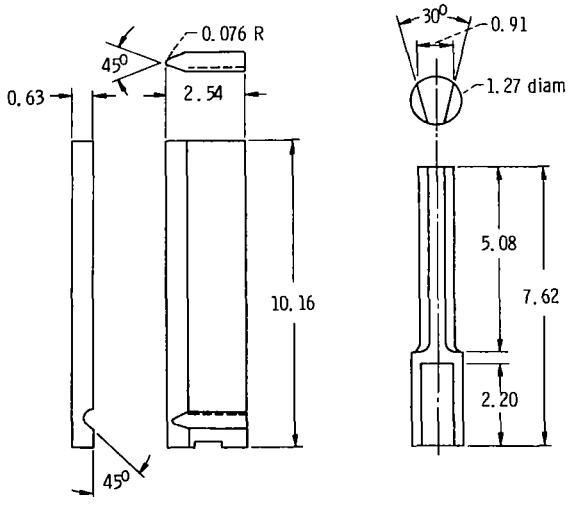

(a) NASA specimen.

(b) Pratt & Whitney specimen.

Figure 1. - High-gas-velocity oxidation specimens. (Dimensions are in centimeters.)

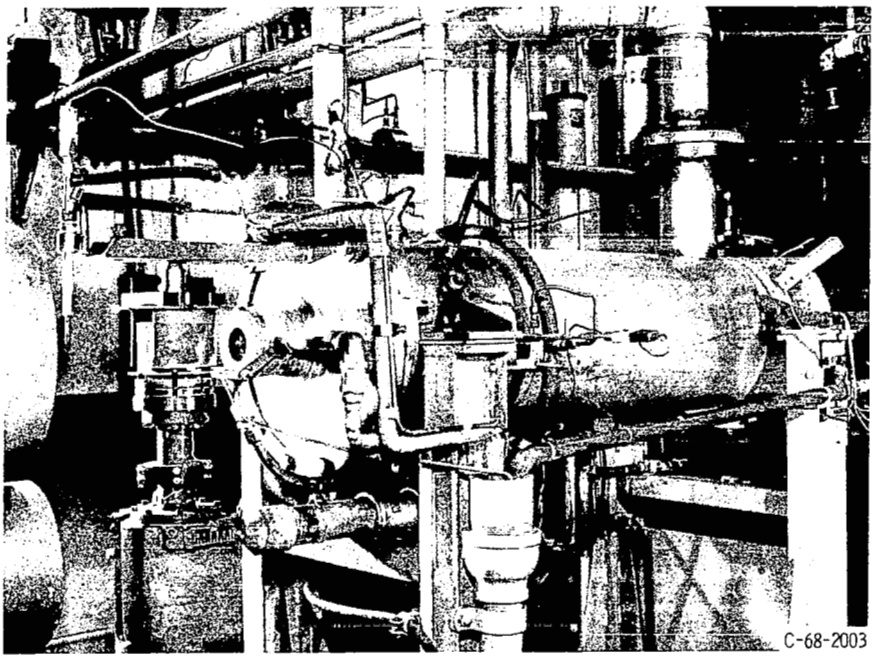

Figure 2. - High-gas-velocity oxidation apparatus.

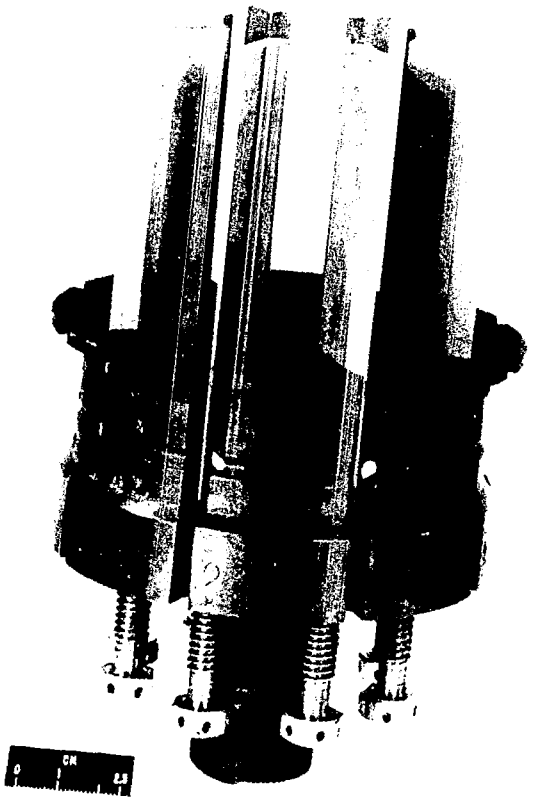

(a) Holder with NASA specimens.

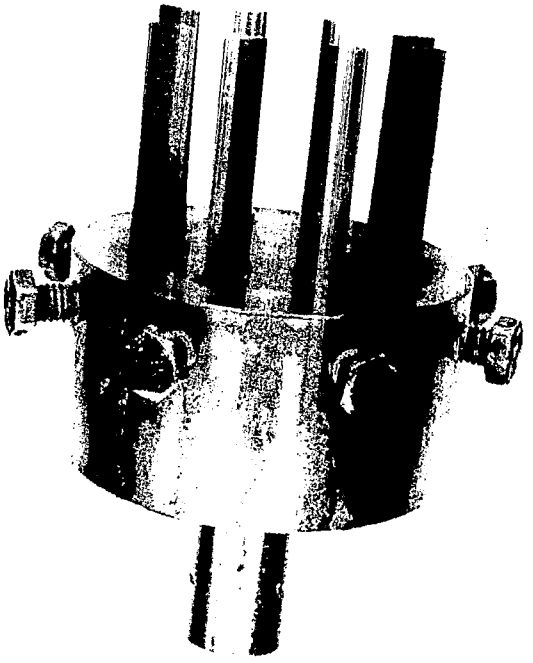

(b) Holder with Pratt & Whitney specimens.

Figure 3. - Specimen holder assemblies.

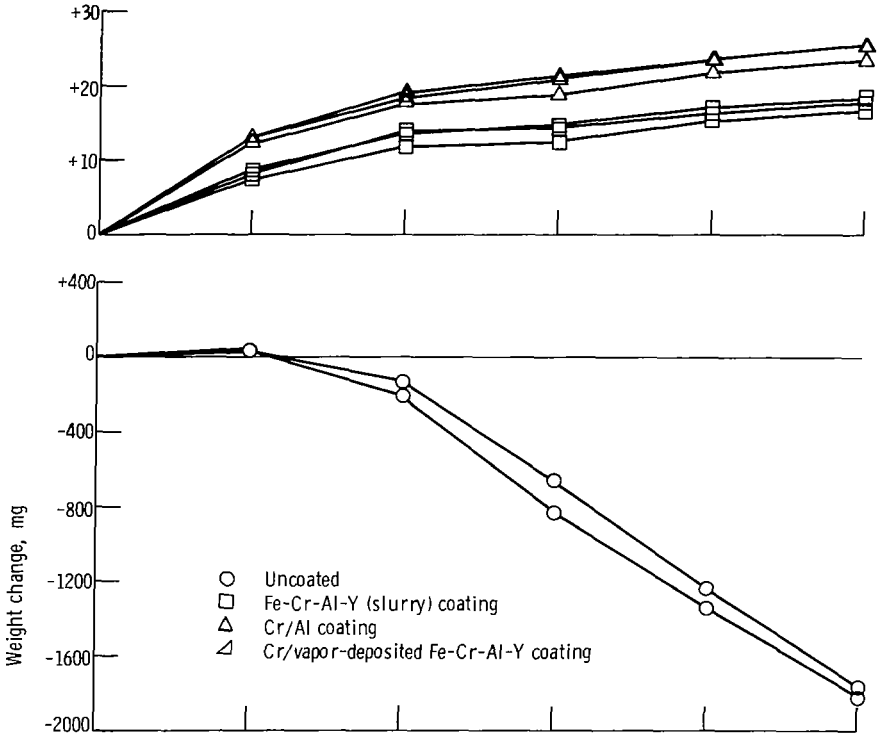

(a) NASA configuration - at 980° C.

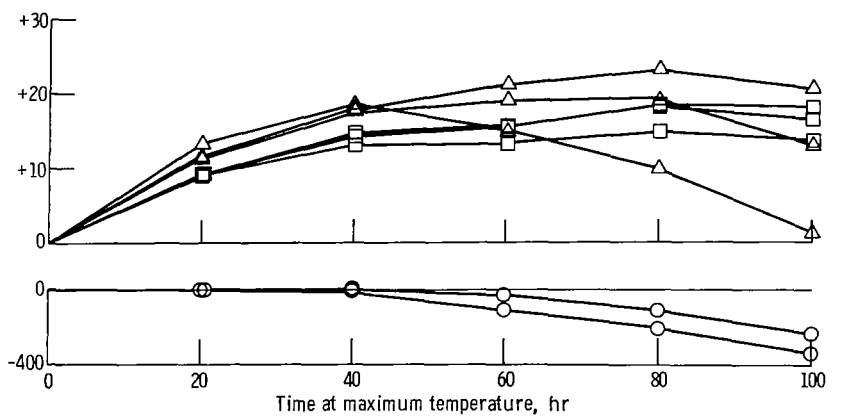

(b) NASA configuration - at 1040° C.

Figure 4. - Weight change of NX-188 specimens of two configurations at various temperatures during exposure to high-gas-velocity oxidation apparatus. Test cycle: 1 hour at test temperature, 3 minutes at room temperature.

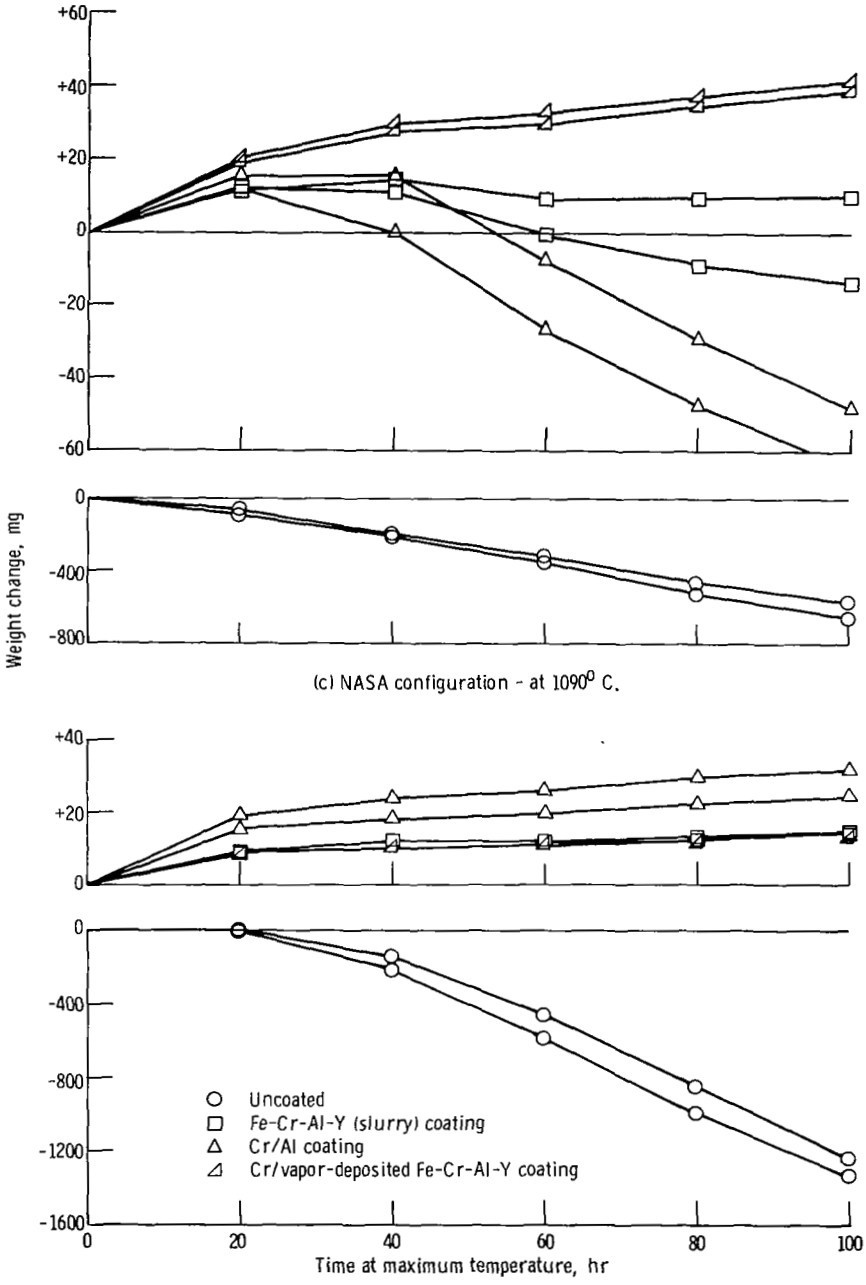

(c) NASA configuration - at 1090° C.

(d) Pratt & Whitney configuration - at 980° C.

Figure 4. - Continued.

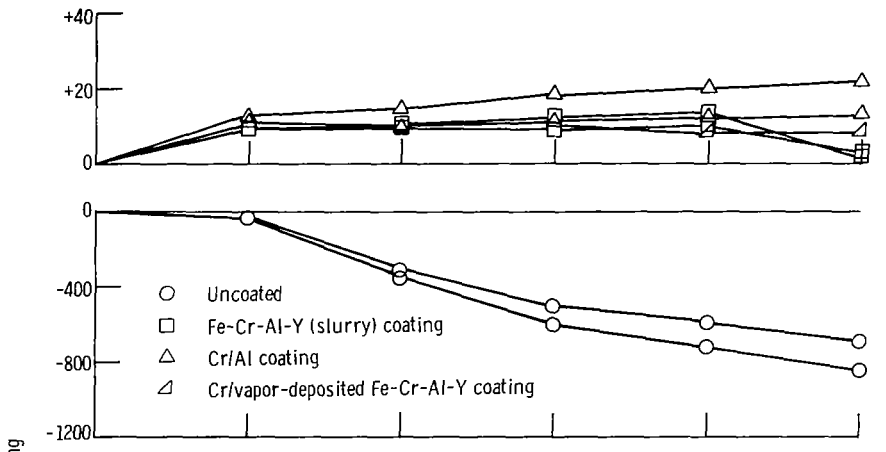

(e) Pratt & Whitney configuration - at 1040° C.

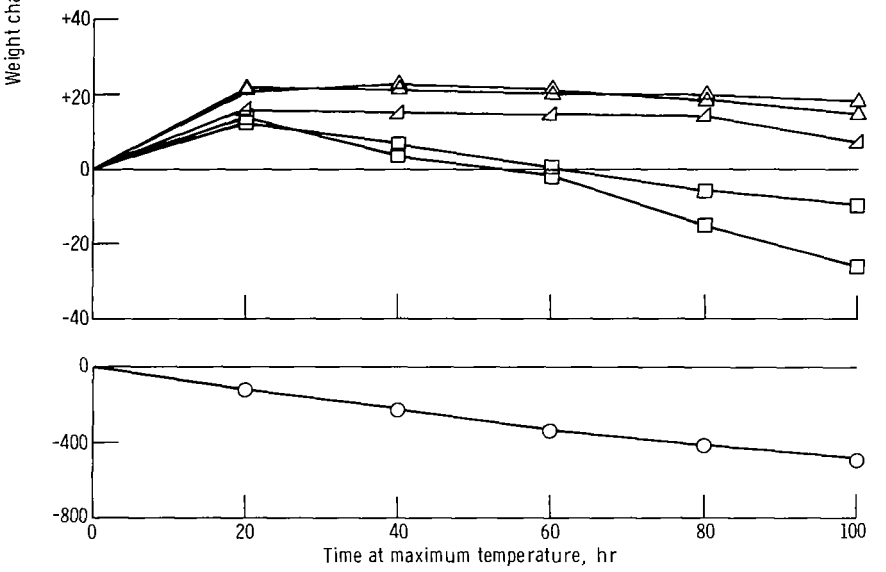

(f) Pratt & Whitney configuration - at 1090° C.

Figure 4. - Concluded.

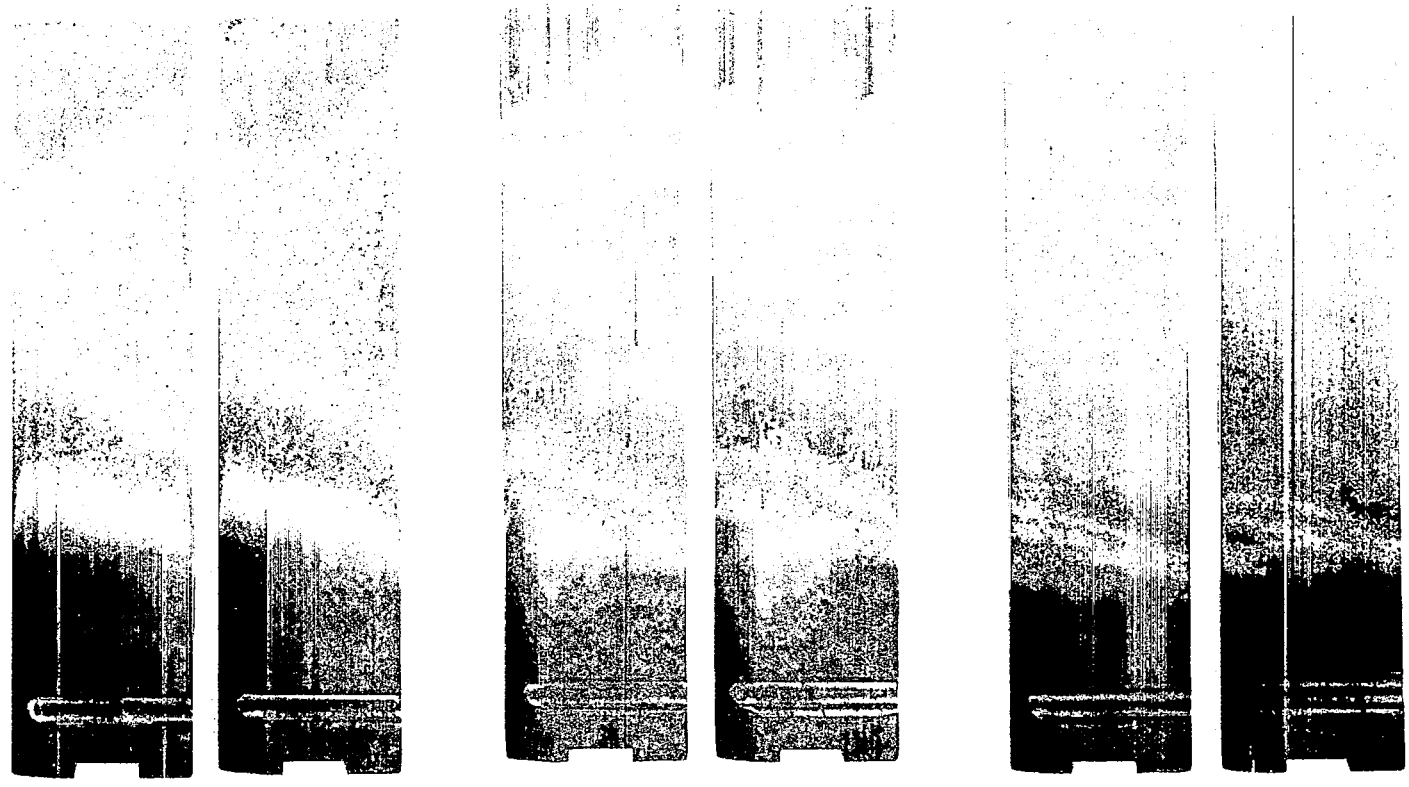

(a) 980° C. (b) 1040° C. (c) 1090° C.

Figure 5. - Uncoated NX-188 specimens after 100-hour exposure in high-gas-velocity oxidation apparatus. Test cycle: 1 hour at test temperature, 3 minutes at room temperature.

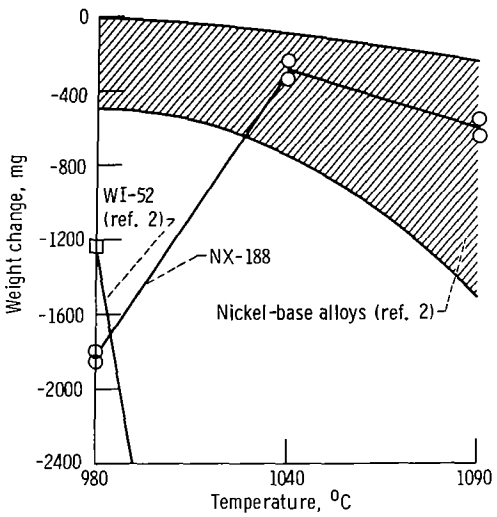

Figure 6. - Effect of test temperature on weight change during exposure to high-gas-velocity oxidation apparatus. Test cycle: 1 hour at test temperature, 3 minutes at room temperature. NASA-type specimens, uncoated NX-188 and representative superalloys.

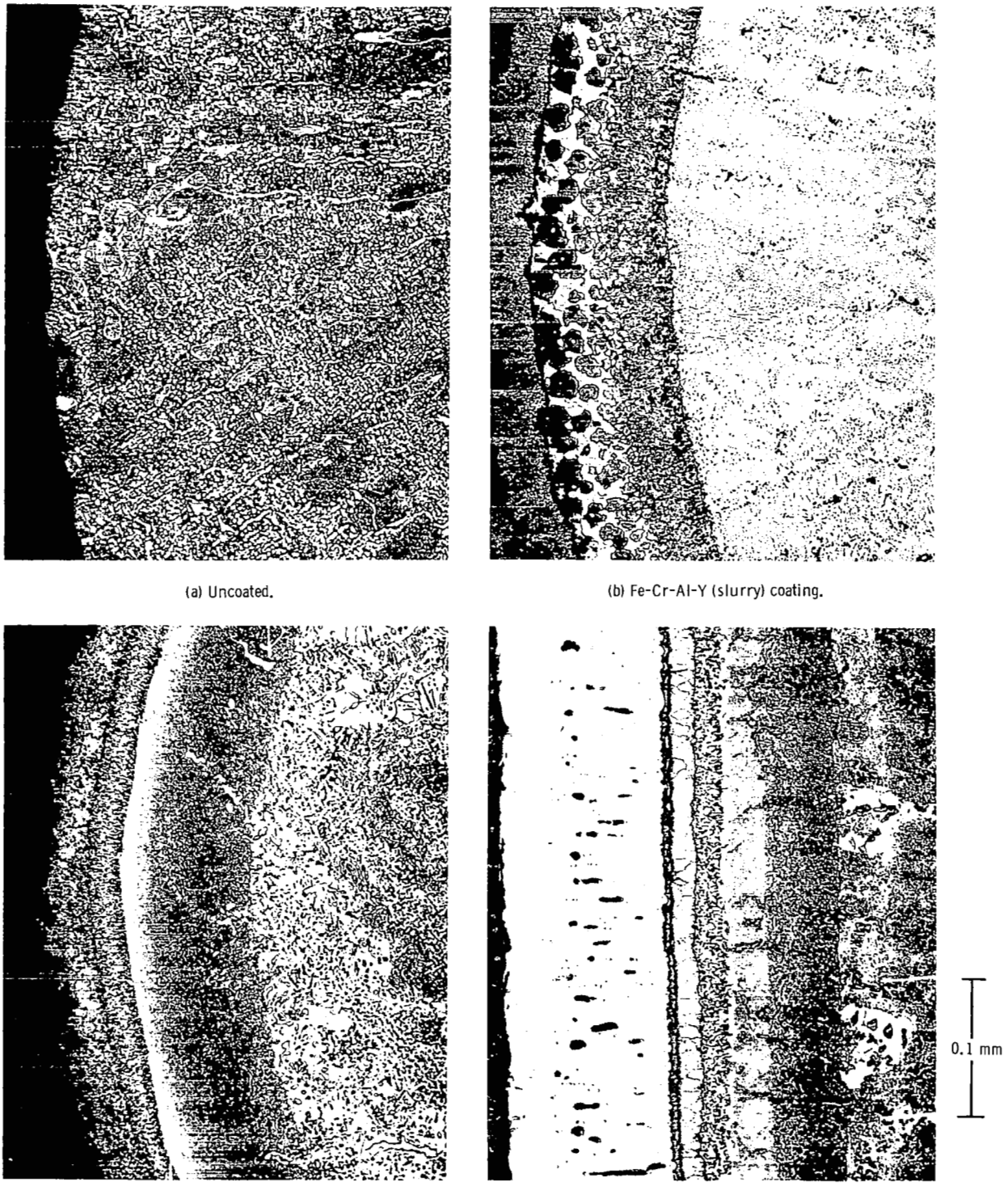

(a) Uncoated.

(b) Fe-Cr-Al-Y (slurry) coating.

(c) Cr/Al coating.

(d) Cr/vapor-deposited Fe-Cr-Al-Y coating.

Figure 7. - Typical microstructures of as-received uncoated and coated NX-188.

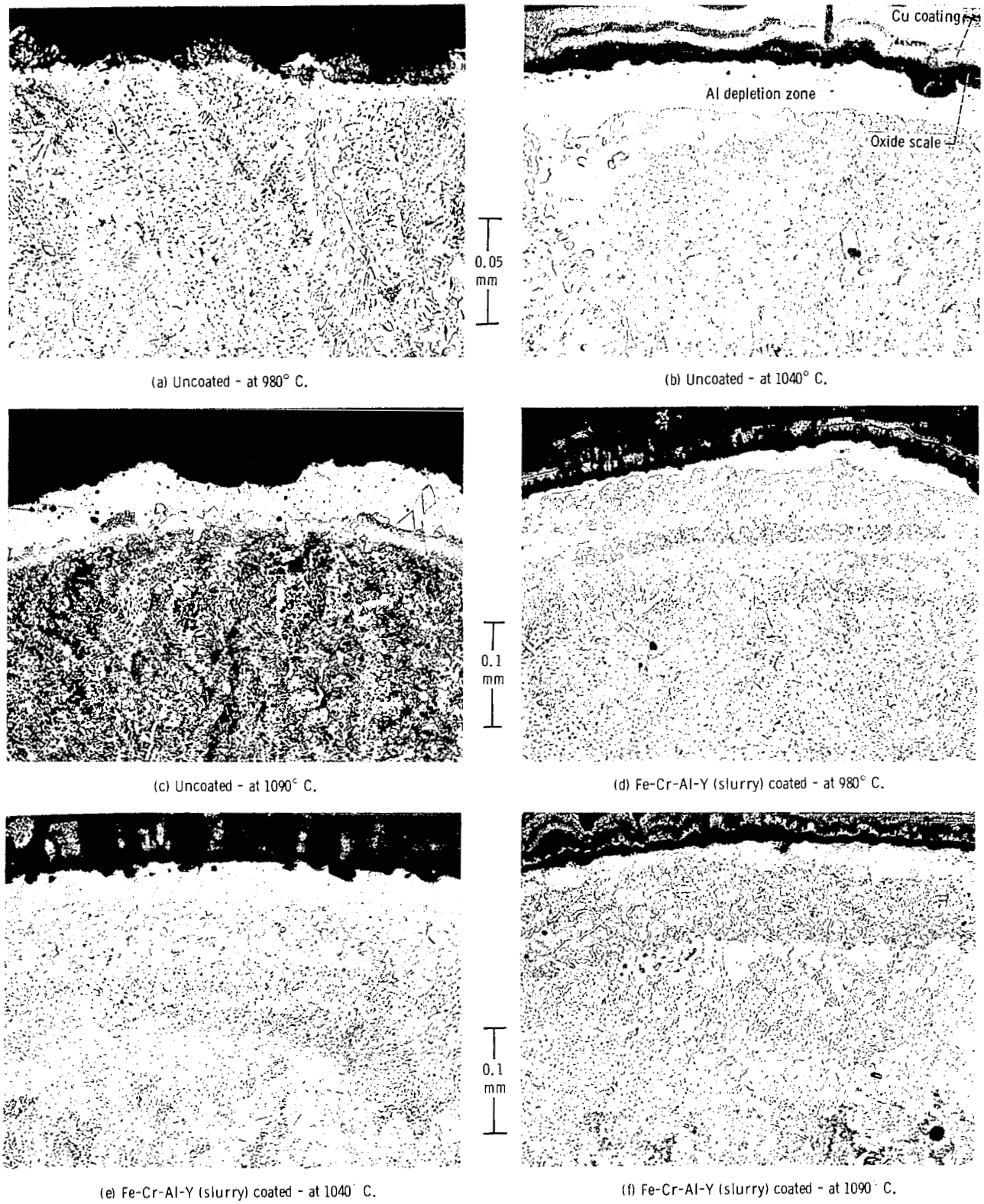

(a) Uncoated - at 980° C.

(b) Uncoated - at 1040° C.

(c) Uncoated - at 1090° C.

(d) Fe-Cr-Al-Y (slurry) coated - at 980° C.

(e) Fe-Cr-Al-Y (slurry) coated - at 1040° C.

(f) Fe-Cr-Al-Y (slurry) coated - at 1090° C.

Figure 8. - Photomicrographs of the leading edges of NX-188 specimens (NASA type) after 100-hour exposure to high-gas-velocity oxidation.

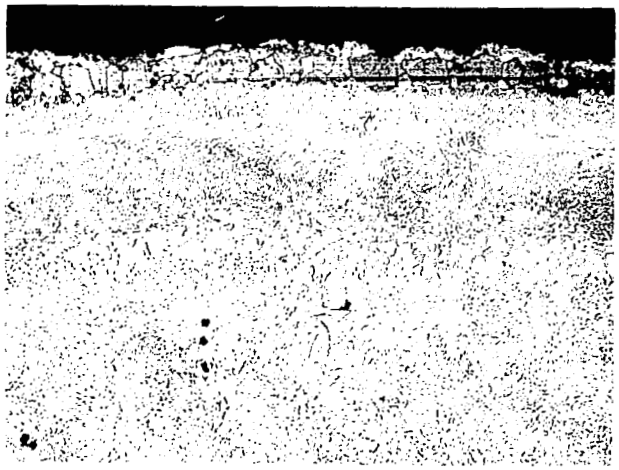

(g) Cr/Al coated - at 980° C.

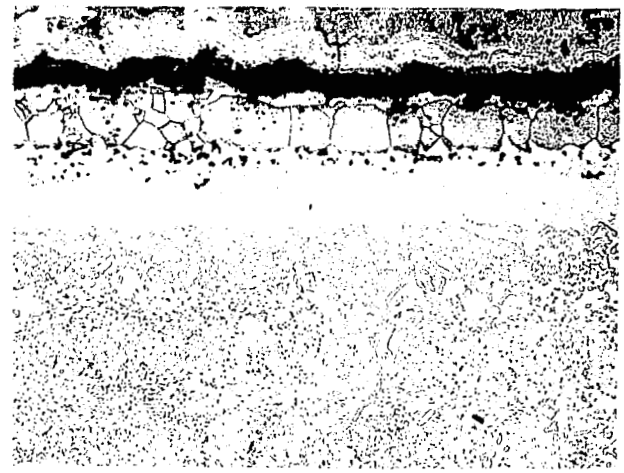

(h) Cr/Al coated - at 1040° C.

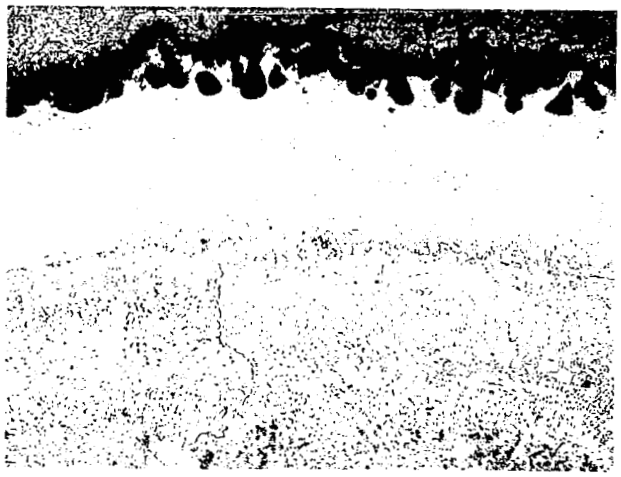

(i) Cr/Al coated - at 1090° C.

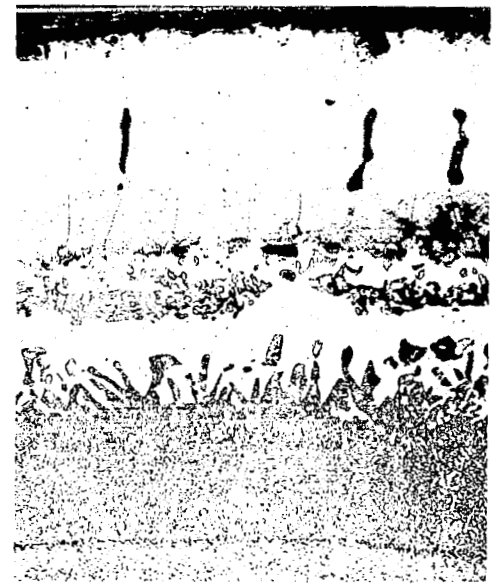

(j) Cr/vapor-deposited Fe-Cr-Al-Y coated - at 1090° C.

Figure 8. - Concluded.

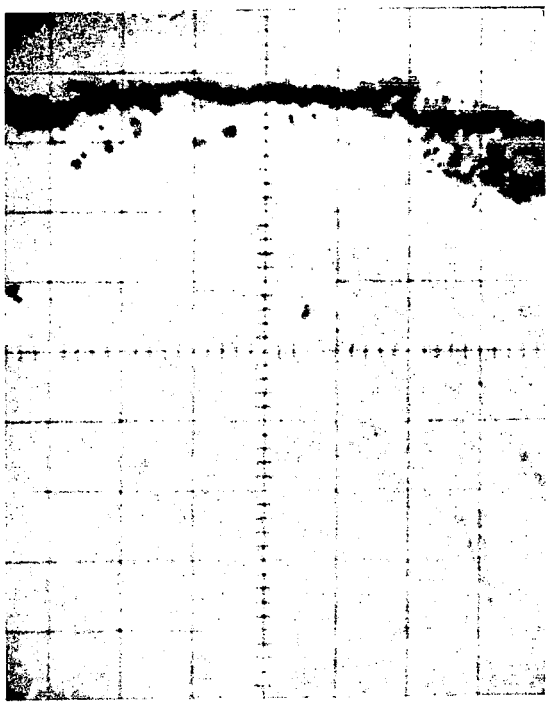

(a) Backscatter electron.

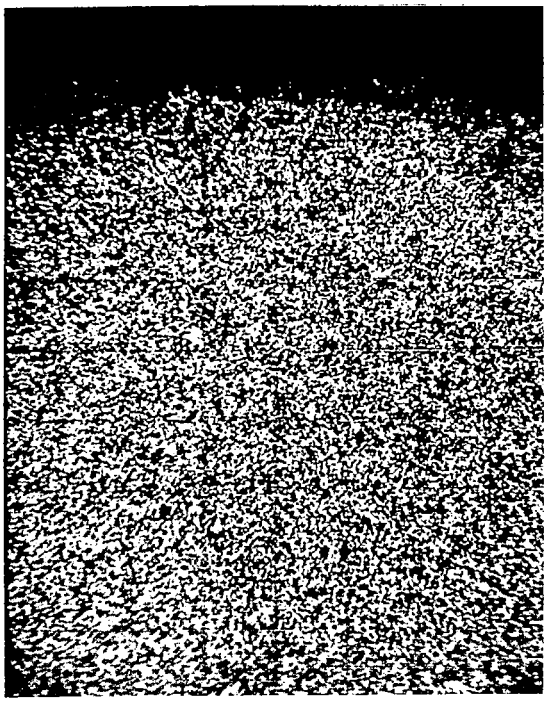

(b) Nickel X-ray.

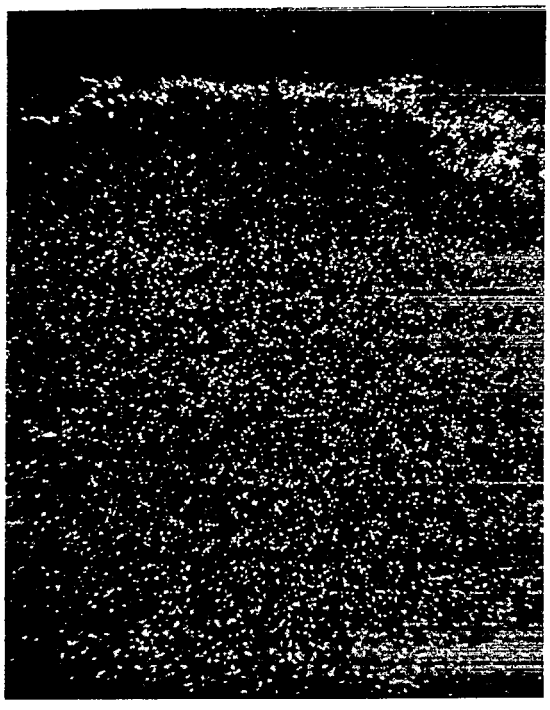

(c) Aluminum X-ray.

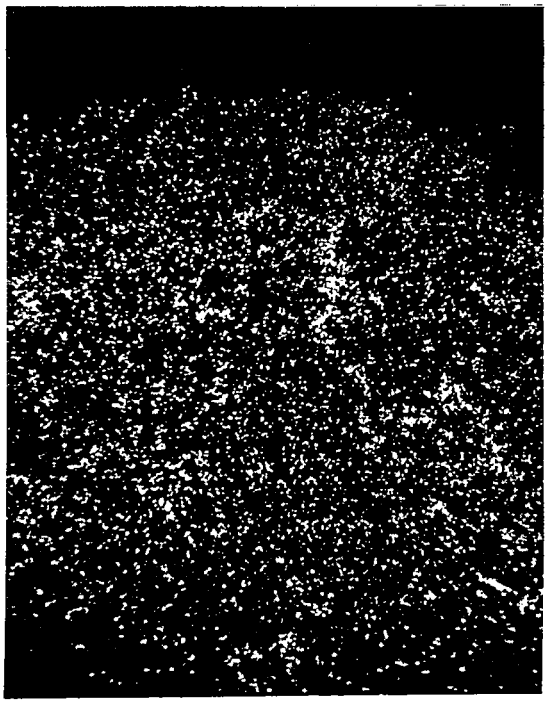

(d) Molybdenum X-ray.

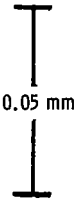

Figure 9. - Electron microprobe X-ray analyzer (EMXA) raster micrographs of uncoated NX-188 specimens after 100-hour exposure to high-gas-velocity oxidation at 1040° C.

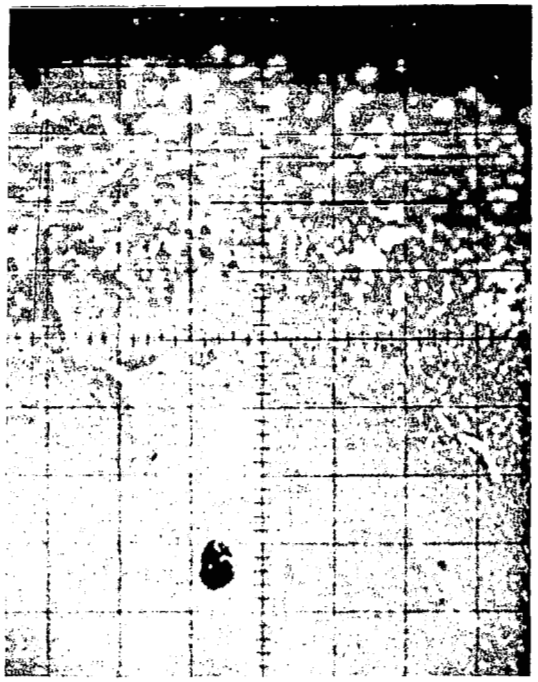

(a) Backscatter electron.

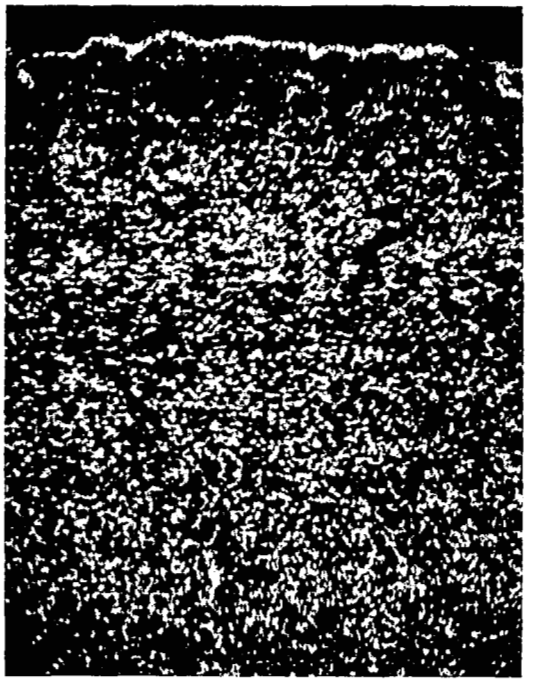

(b) Aluminum X-ray.

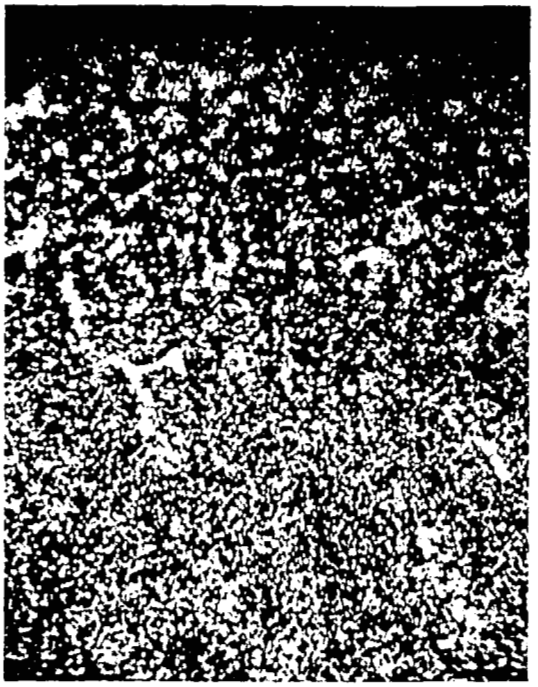

(c) Molybdenum X-ray.

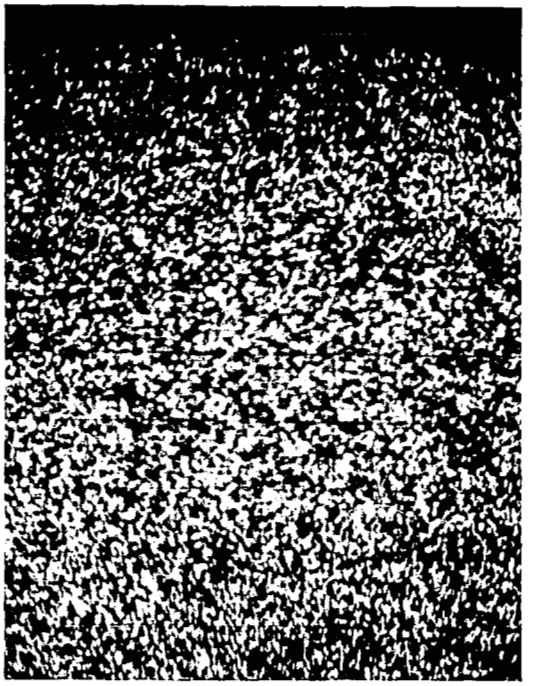

(d) Nickel X-ray.

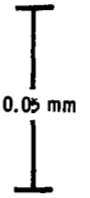

Figure 10. - EMXA raster micrographs of Fe-Cr-Al-Y (slurry) coated NX-188 specimens after 100-hour exposure to high-gas-velocity oxidation at 980° C.

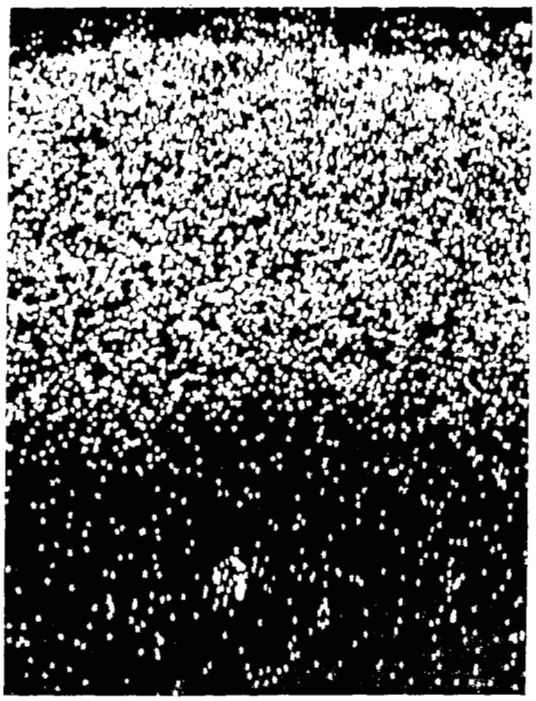

(e) Chromium X-ray.

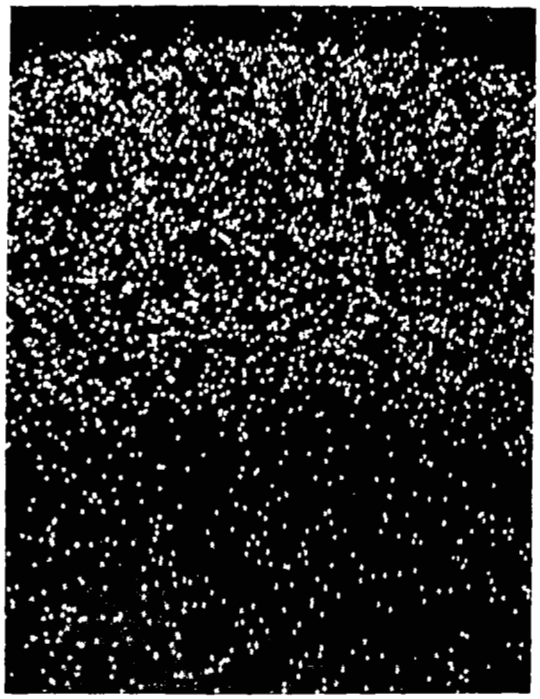

(f) Iron X-ray.

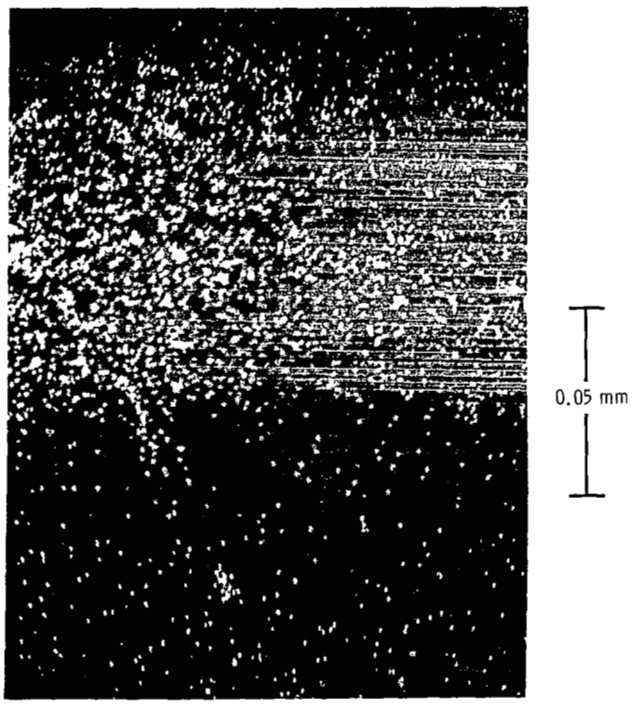

(g) Silicon X-ray.

Figure 10. - Concluded.

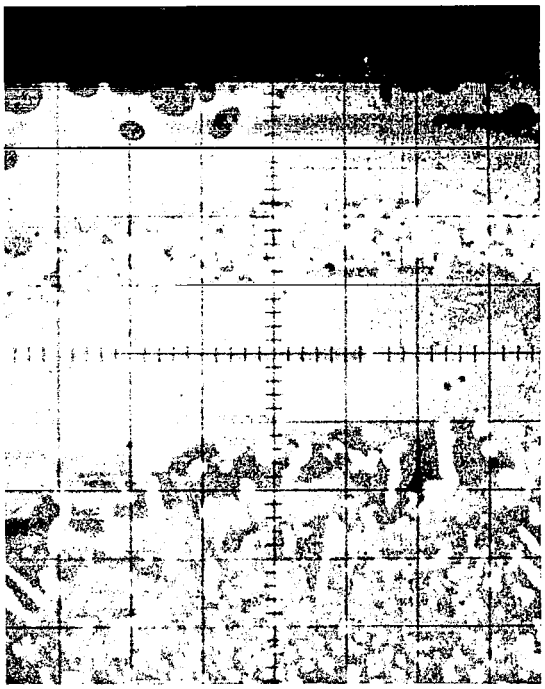

(a) Backscatter electron.

(b) Aluminum X-ray.

(c) Molybdenum X-ray.

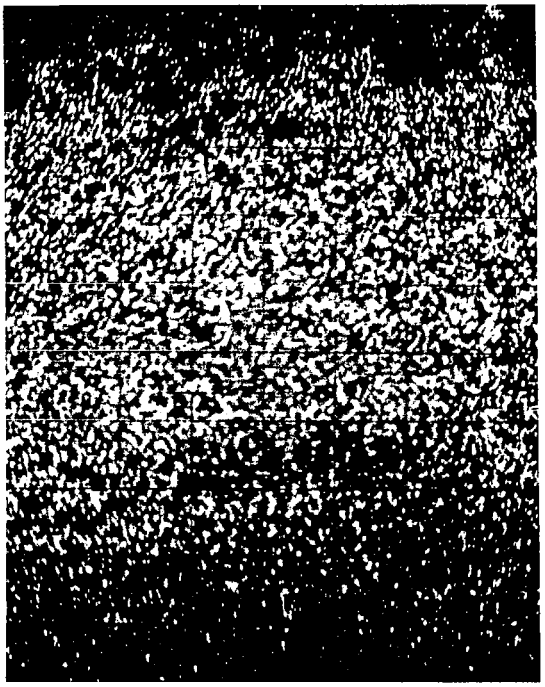

(d) Chromium X-ray.

0.05 mm

Figure 11. - EMXA raster micrographs of Cr/Al (pack) coated NX-188 specimens after 100-hour exposure to high-gas-velocity oxidation at 1090° C.

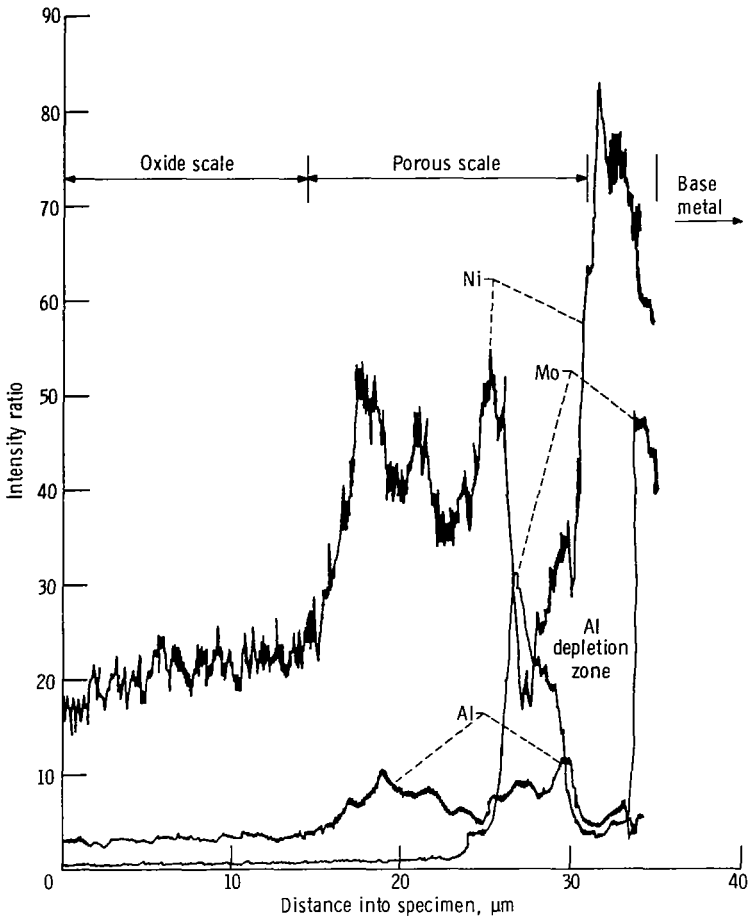

Figure 12. - Typical electron microprobe X-ray analyzer (EMXA) element concentration profile. Uncoated NX-188 specimen after 100-hour exposure to high-gas-velocity oxidation at 980° C.

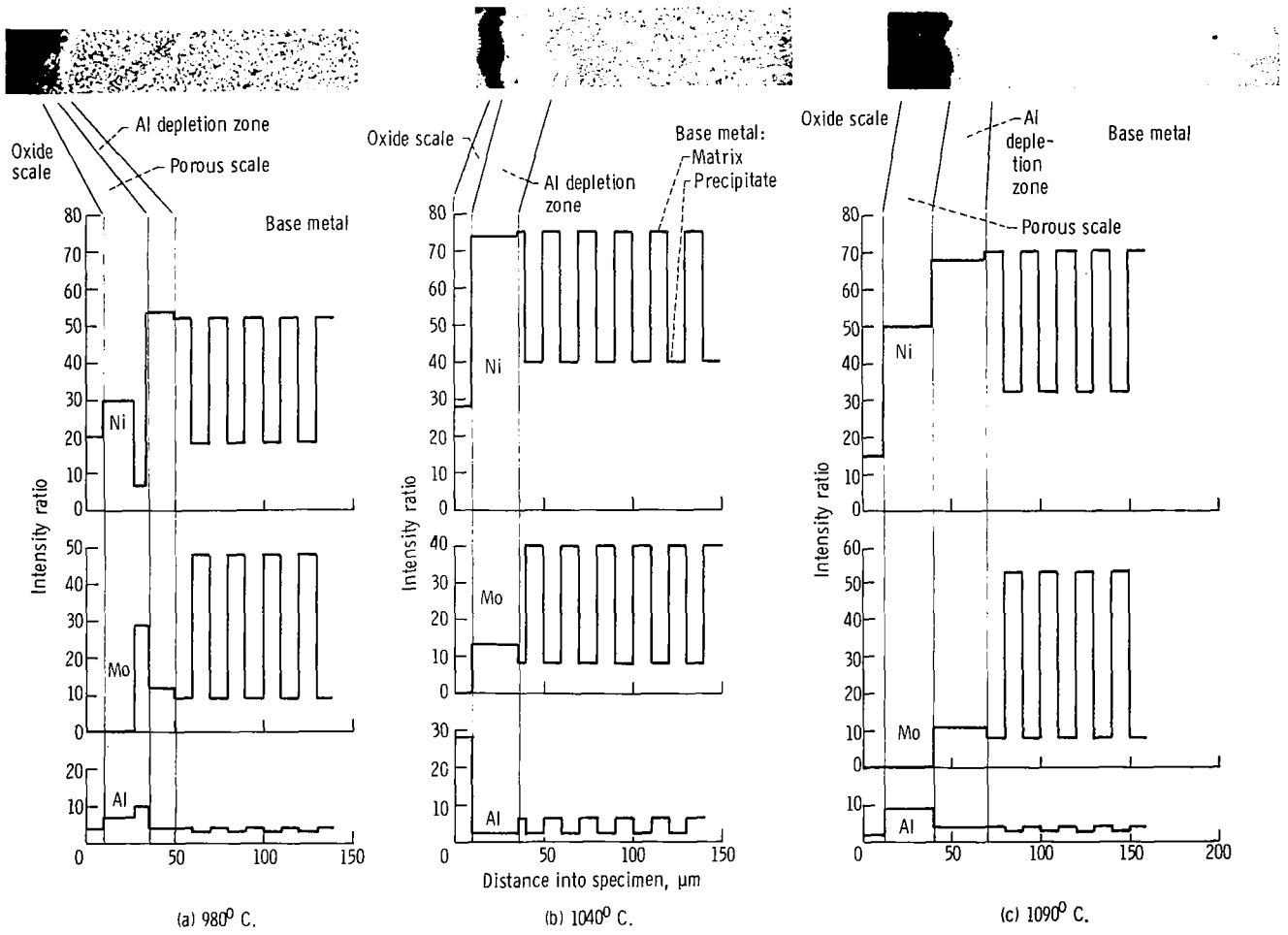

Figure 13. - Schematic representation of EMXA concentration profile data for uncoated NX-188 specimen after 100-hour exposure to high-gas-velocity oxidation.

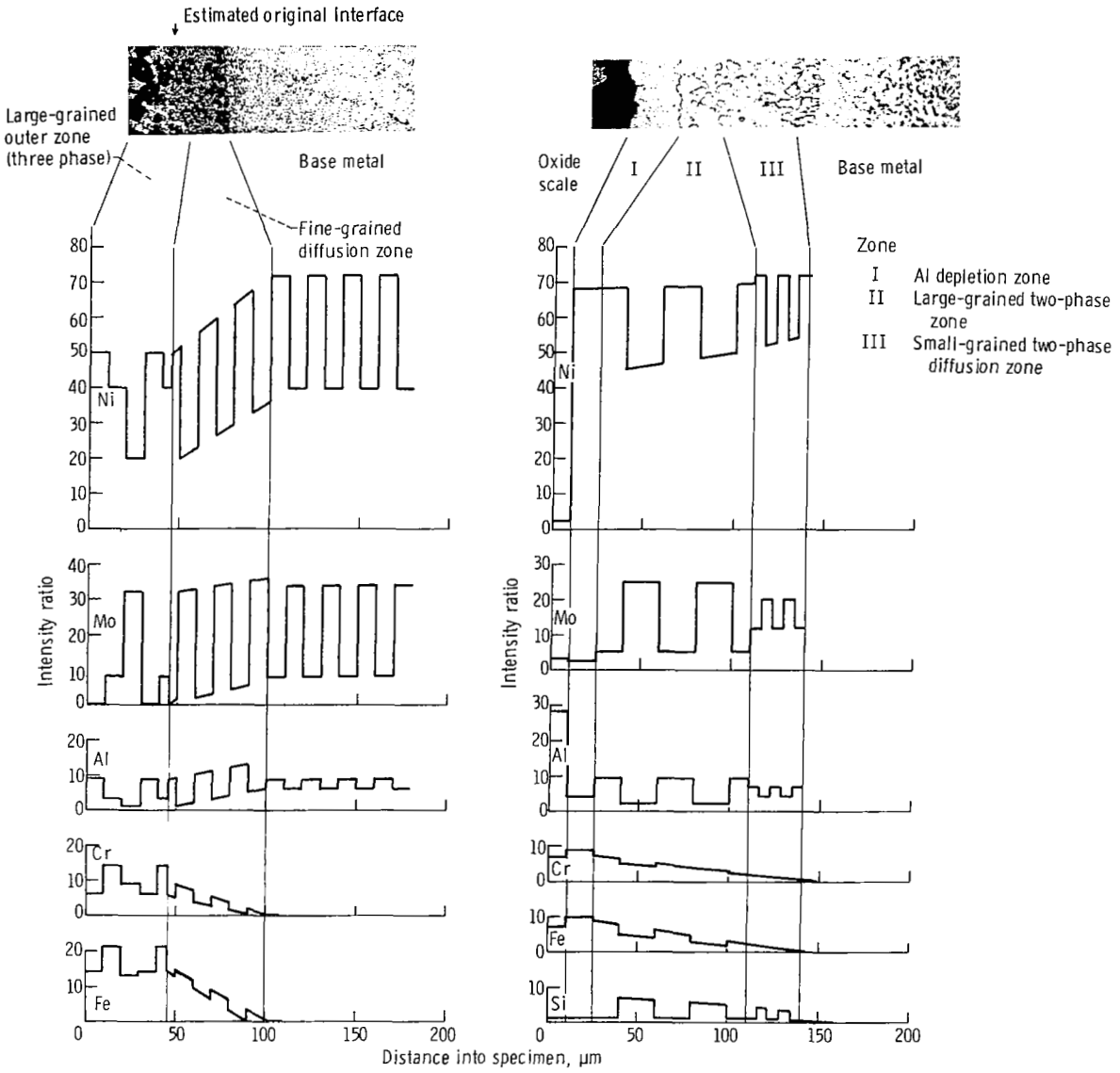

Figure 14. - Schematic representation of EMXA concentration profile data for Fe-Cr-Al-Y (slurry) coated NX-188 specimen.

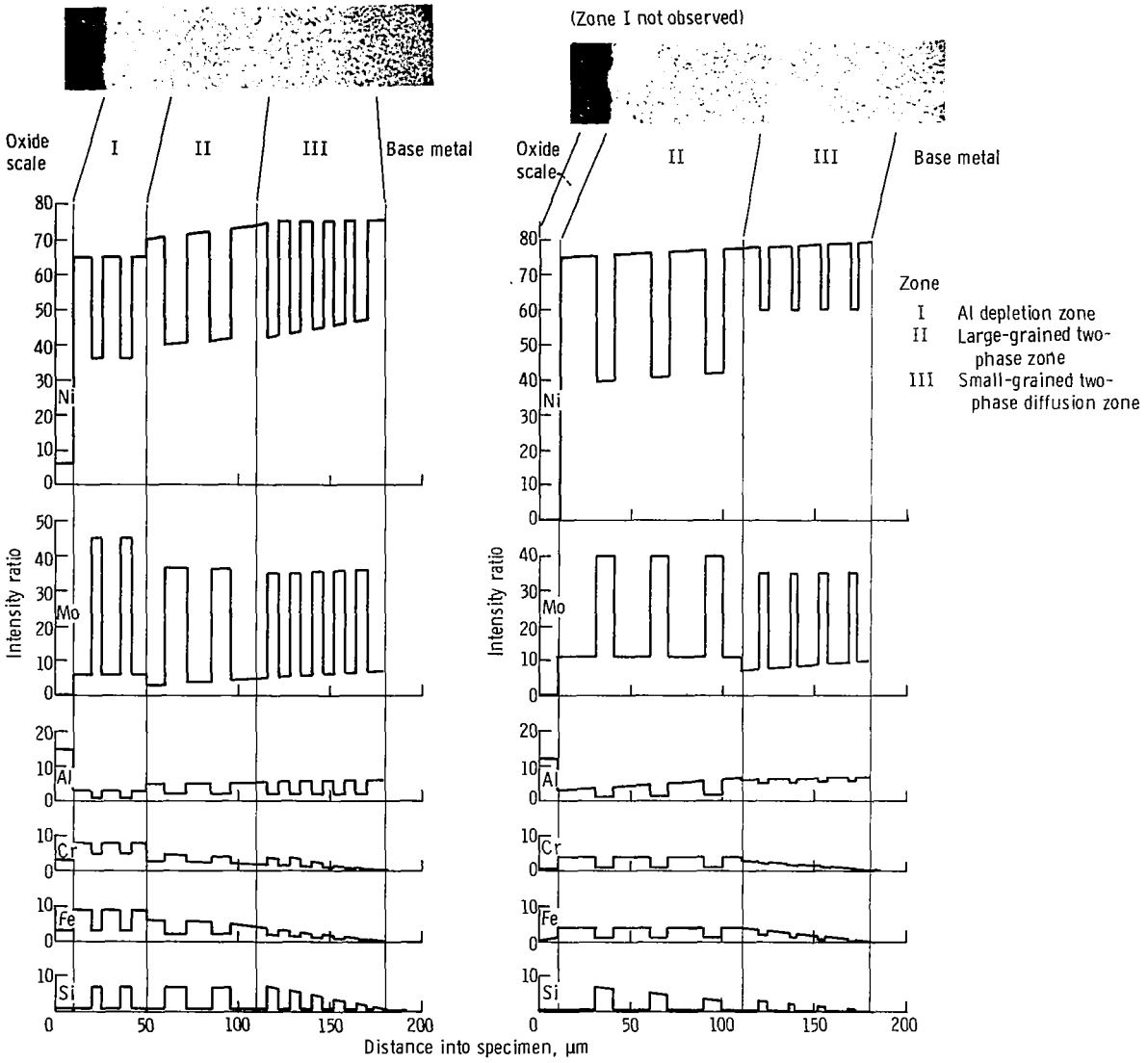

(c) After 100-hour exposure to high-gas-velocity oxidation at 1040° C.

(d) After 100-hour exposure to high-gas-velocity oxidation at 1090° C.

Figure 14. - Concluded.

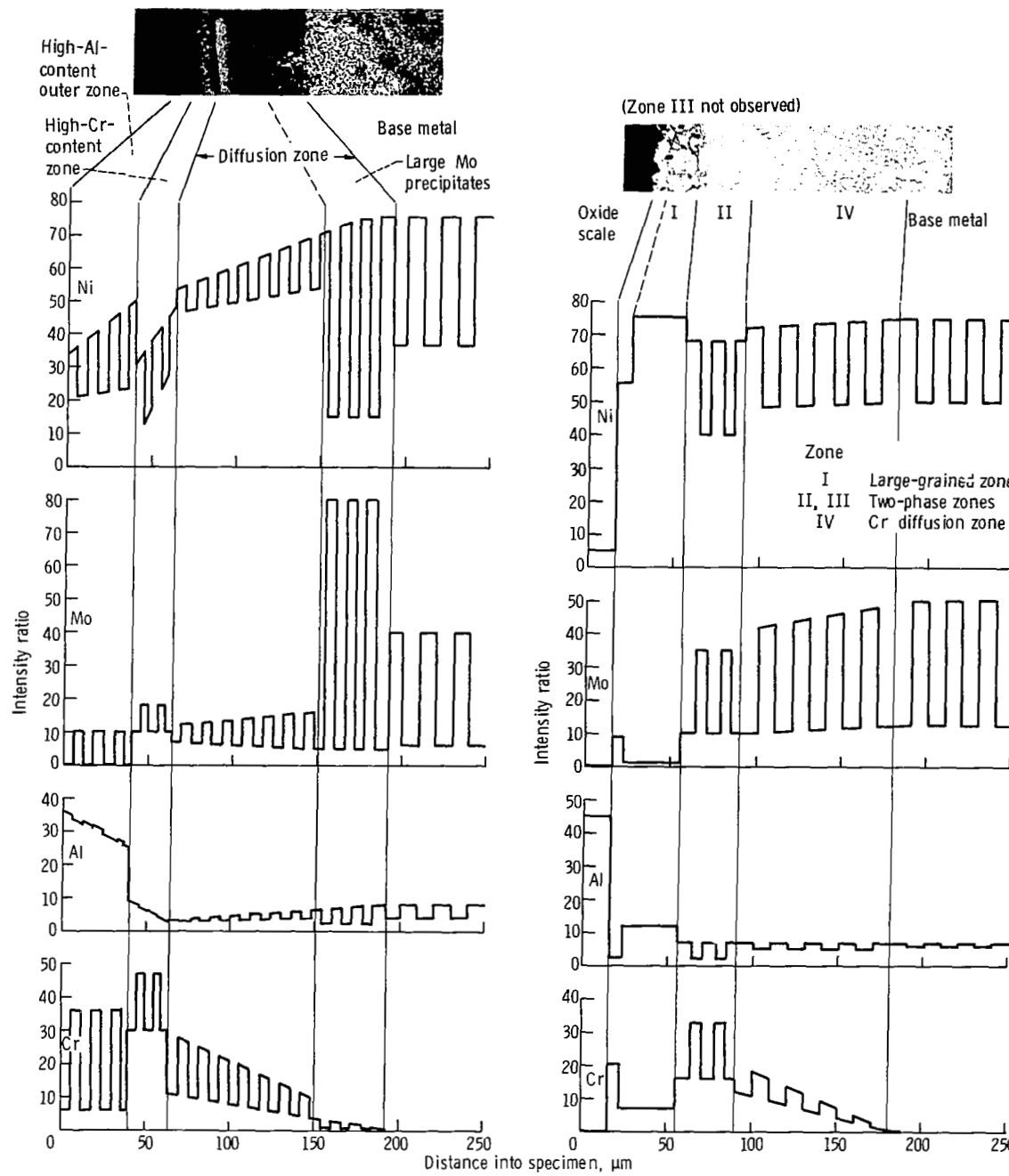

(a) As received.

(b) After 100-hour exposure to high-gas-velocity oxidation at 980° C.

Figure 15. - Schematic representation of EMXA concentration profile data for Cr/Al (pack) coated NX-188 specimen.

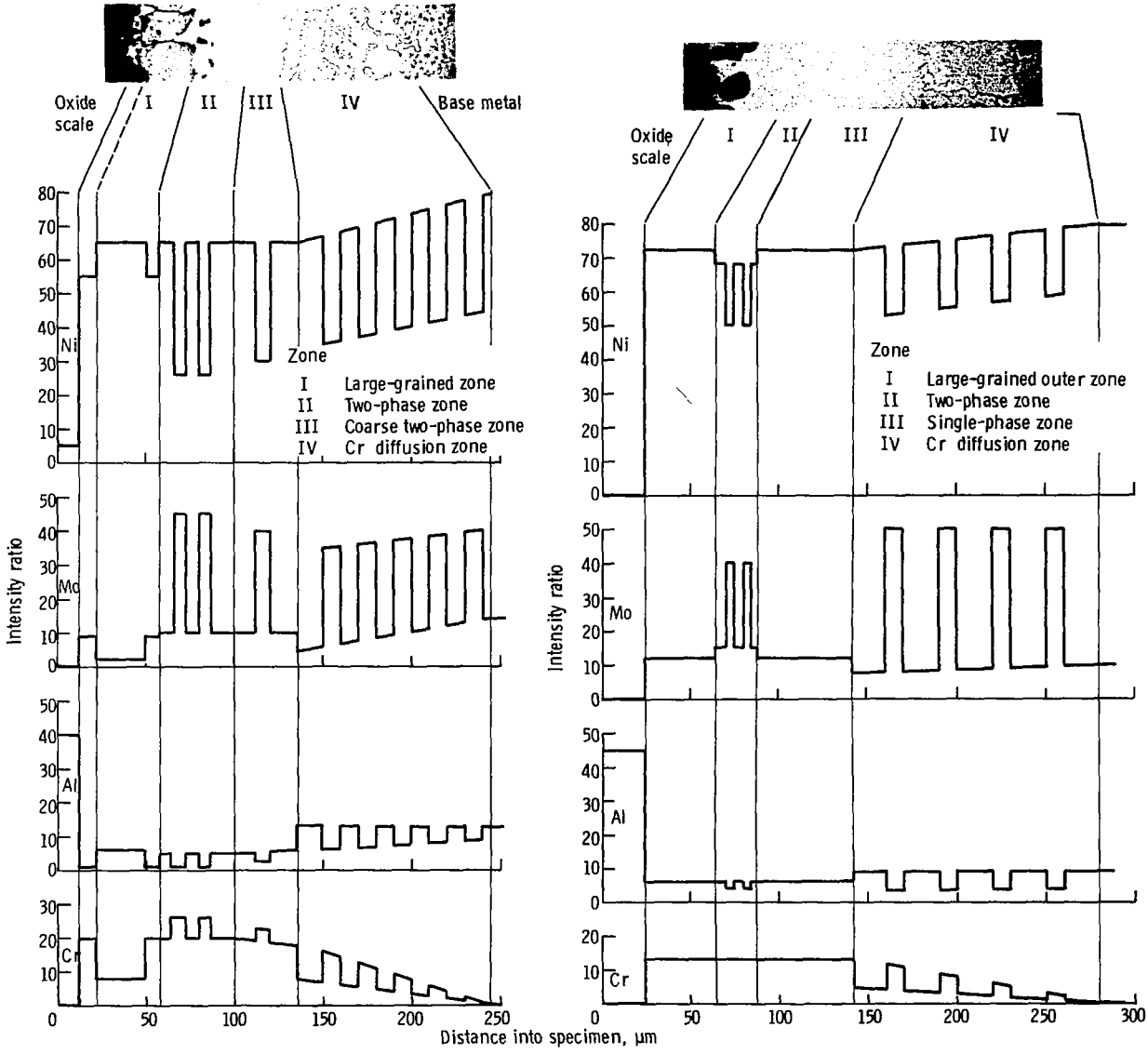

(c) After 100-hour exposure to high-gas-velocity oxidation at 1040° C.

(d) After 100-hour exposure to high-gas-velocity oxidation at 1090° C.

Figure 15. - Concluded.

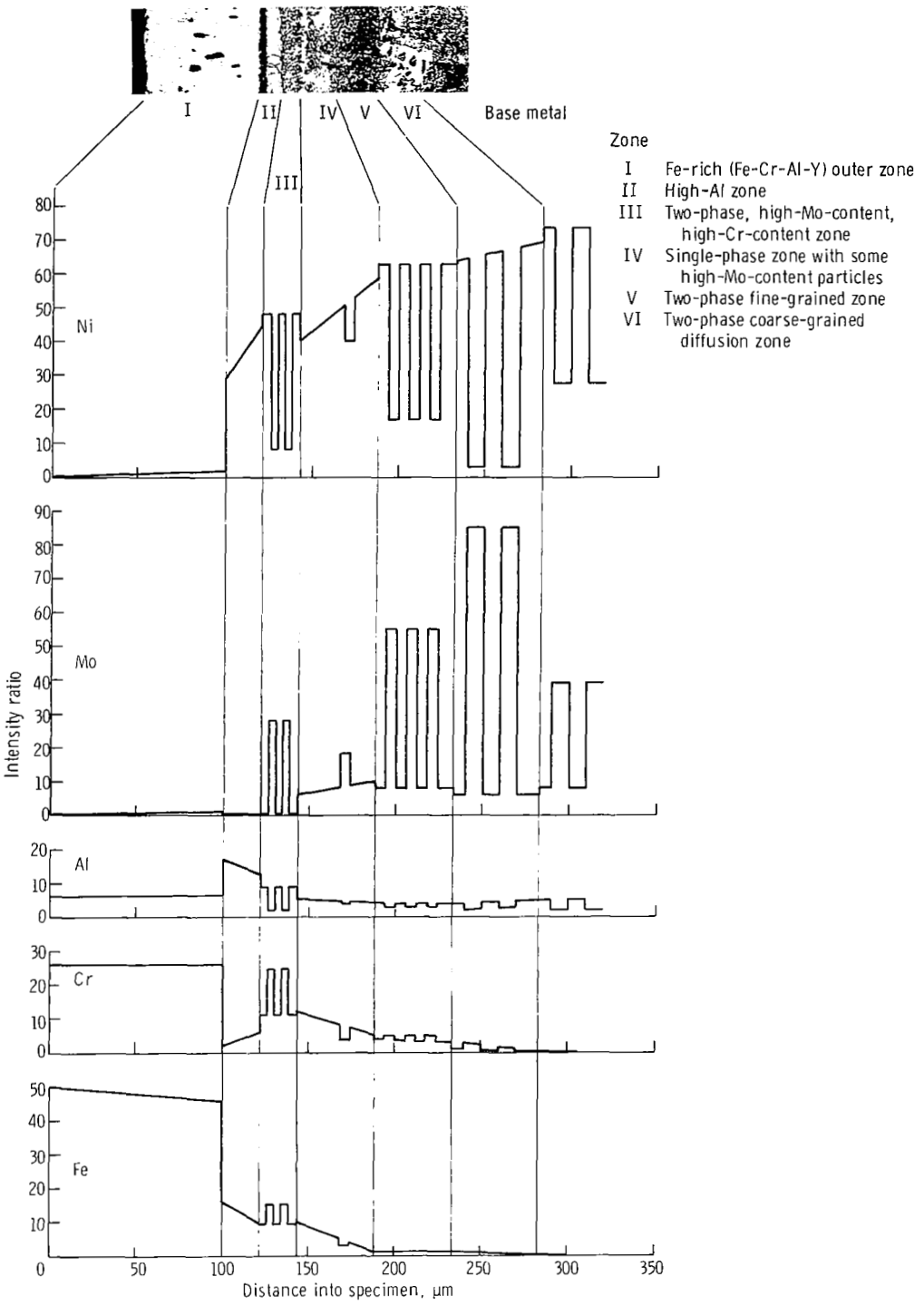

(a) As received.

Figure 16. - Schematic representation of EMXA concentration profile data for Cr vapor-deposited Fe-Cr-Al-Y coated NX-188 specimen.

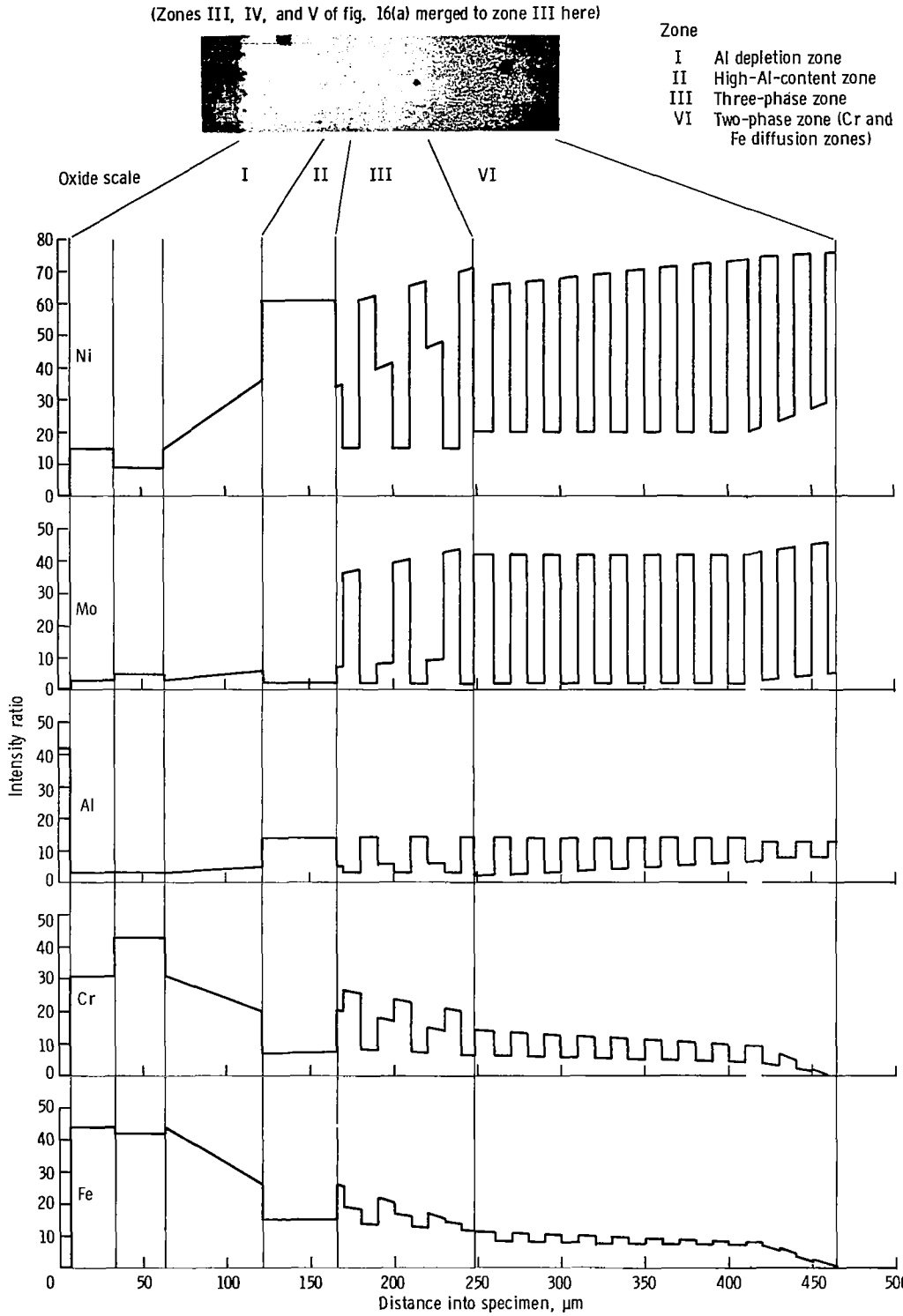

(b) After 100-hour exposure to high-gas-velocity oxidation at 1090° C.

Figure 16. - Concluded.